72 °C. The mRNA expression of target genes was normalized by using the mRNA level of GAPDH.

2.5. Effect of shRNA-expressing pDNAs on proliferation of B16 cells

B16-BL6/dual Luc cells were transfected with pDNA as described above. After the transfection of pDNAs for 4 h, cells were washed with PBS and further incubated with the culture medium for specified time periods up to 96 h. The cell numbers at the indicated time points were evaluated by MTT assay as described previously [25].

2.6. Flow cytometric determination of apoptosis

B16-BL6/dual Luc cells seeded on 6-well culture plates were treated with pDNA as described above. At 3 days after transfection, adherent cells were detached by trypsinization and re-suspended in PBS. Aliquots of these cell suspensions were centrifuged and the pellets were used for the flow cytometric determination of apoptosis using a commercial kit (Vybrant™ Apoptosis Assay Kit #2, Molecular Probes, Invitrogen). In brief, a cell pellet was re-suspended in a binding buffer (10 mM HEPES, 140 mM NaCl, 2.5 mM $CaCl_2$, pH 7.4) to give a cell density of approximately $2–10\times10^5$/ml. Aliquots (100 μl) of this cell suspension were incubated with 5 μl recombinant annexin V labeled with Alexa Fluor® 488 dye (Alexa Fluor 488 annexin V) and 1 μl of a stock solution of propidium iodide (PI, 100 μg/ml) for 15 min at room temperature. After the incubation period, 400 μl of the binding solution was added and the samples were kept on ice until analysis in the flow cytometer. Samples were analyzed on a flow cytometer (FACSCan, BD, Franklin Lakes, NJ, USA) and electronic compensation was used to remove spectraloverlap. Annexin V staining, DNA signals and side scatter (SSC) signals were detected on a log scale. Forward (FSC) signals were detected in a linear mode. The FL1 and FL2 photomultiplier (PMT) voltage settings were set using unstained isotype samples. The threshold using FSC was set to exclude debris without excluding any populations of interest. The flow cytometric data were analyzed with WINMDI 2.8 software®.

2.7. Animals

Seven-week-old male C57/BL6 mice, purchased from Shizuoka Agricultural Cooperative Association (Shizuoka, Japan) were used in all the experiments. All animal experiments were conducted in accordance with the principles and procedures outlined in the US National Institutes of Health Guide for the Care and Use of Laboratory Animals. The protocols for animal experiments were approved by the Animal Experimentation Committee of Graduate School of Pharmaceutical Sciences of Kyoto University.

2.8. Primary tumor model

B16-BL6 cells in an exponential growth phase were harvested by trypsinization and suspended in Hanks' balanced salt solution (HBSS, Nissui Pharmaceutical). The tumor cells (2×10^5 cells) were injected intradermally into the back of syngeneic C57/BL6 mice. When the tumor diameter reached 2–3 mm (1 week after tumor inoculation), mice received a single intratumoral injection of 30 μg pDNA dissolved in 50 μl saline at a time followed by twelve electric pulses (1000 V/cm, 5 ms, 4 Hz) which were delivered through a pair of 1-cm^2 forcep-type electrodes connected to a rectangular direct current generator (CUY21, Nepagene, Chiba, Japan). In the growth inhibition experiment, shRNA-expressing pDNAs were administrated at day 7, 10 and 19 after tumor inoculation. Tumor growth was evaluated by measuring the tumor size using calipers at indicated times, and tumor volume (mm^3) was calculated from the following equation: $(\text{longest diameters}\times\text{shortest diameters})^{3/2}\times\pi/6$.

2.9. Statistical analysis

Differences were statistically evaluated by Student's *t*-test. A *P*-value of less than 0.05 was considered to be statistically significant.

3. Results

3.1. Reduction in mRNA by transfection of shRNA-expressing pDNA to B16-F1 cells

Two candidate sequences were selected for each target gene. Fig. 1 shows the mRNA levels of the target genes in B16-F1 cells 24 h after transfection of shRNA-expressing pDNA targeting β-catenin or HIF1α measured by real-time RT-PCR. The transfection of shRNA-expressing pDNA maximally suppressed the mRNA expression of β-catenin and HIF1α to about 20% and 25% of each control value, respectively. For each target gene, an shRNA-expressing pDNA (#2 in all cases)

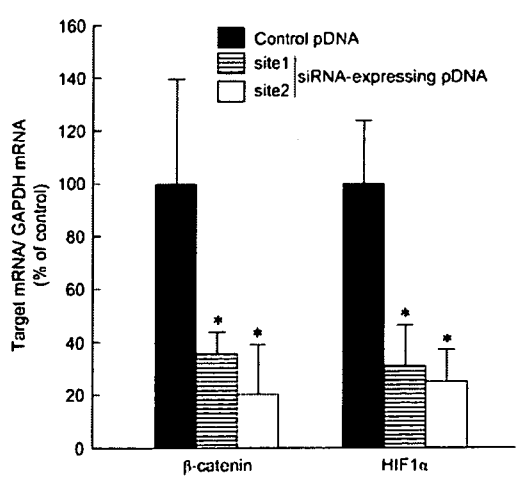

Fig. 1. Reduction of mRNA in B16 cells following transfection of shRNA-expressing pDNA. B16-F1 cells seeded on 12-well culture plates (at a density of 2×10^5 cells/well) were transfected with shRNA-expressing pDNA or piGENE-hU6. Amounts of mRNA were determined 24 h after transfection. The results are expressed as the mean±S.D. ($n=3$). *$P<0.05$ for Student's *t*-test versus control group.

was selected based on the inhibitory effect, and was used in the subsequent experiments. The selected shRNA-expressing pDNAs were named as pshβ-catenin and pshHIF1α.

3.2. Growth inhibition of B16-BL6/dual Luc cells by shRNA-expressing pDNA

To evaluate the inhibitory effect of shRNA-expressing pDNA on tumor cell growth in vitro, the time course of the number of B16-BL6/dual Luc cells after the transfection of shRNA-expressing pDNAs was measured by MTT assay (Fig. 2). Transfection of pshβ-catenin or pshHIF1α reduced the number of viable B16 cells to about 50% and 60% of the control value, respectively. A significant reduction in the viable cell number was observed in the pshβ-catenin- or pshHIF1α-treated cells as early as 1 and 2 days after transfection, respectively. Therefore, these results indicate that pshβ-catenin and pshHIF1α are potent in inhibiting the proliferation of B16 cells.

3.3. Flow cytometric analysis of cell death induced by shRNA-expressing pDNAs

Flow cytometric analysis of cells stained with fluorescein-labeled annexin V and PI was performed to detect apoptotic and necrotic cells after transfection of shRNA-expressing pDNAs to B16-BL6/dual Luc cells (Fig. 3). At 3 days after transfection of shRNA-expressing pDNA, cells were stained with annexin-FITC and PI. Fig. 3A–C shows the typical results of the flow cytometric analysis of the cells. Live cells (annexin-FITC and PI double negative) occupy the lower left quadrant, early apoptotic cells (annexin-FITC positive and PI negative) occupy the lower right quadrant and late apoptotic or necrotic cells (annexin-FITC and PI double positive) occupy the upper right quadrant. Fig. 3D summarizes the number of viable, early apoptotic, or late apoptotic and necrotic cells. Transfection of pshβ-catenin or pshHIF1α increased the number of apoptotic cells compared with that of control pDNA. The number of dead cells, which

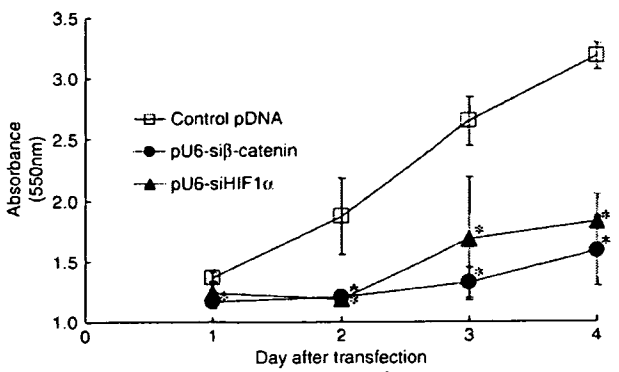

Fig. 2. Anti-proliferative effect of shRNA-expressing pDNA against B16 cells. B16-BL6/dual Luc seeded on 24-well culture plates (at a density of 2×10^4 cells/well) were transfected with shRNA-expressing pDNA or piGENE-hU6. Cell populations at indicated time points were evaluated by MTT Assay. The results are expressed as the mean±S.D. ($n=3$). *$P<0.05$ for Student's t-test versus control group.

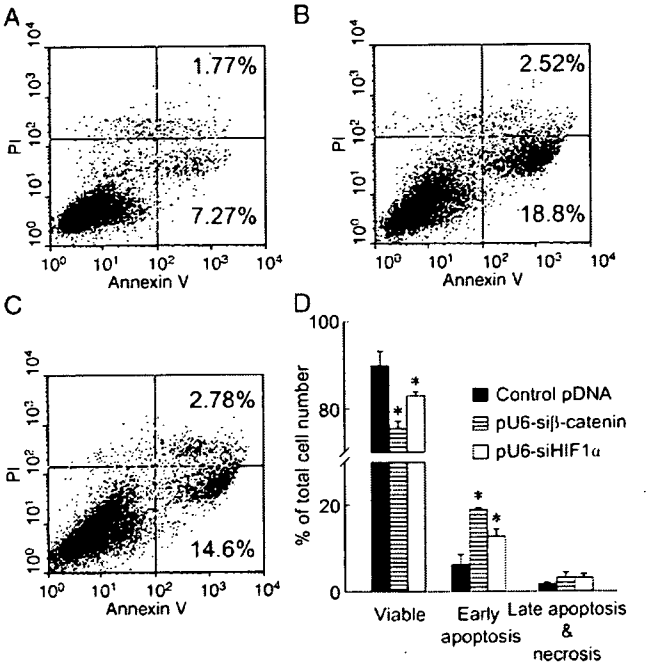

Fig. 3. Induction of apoptosis and necrosis in B16-BL6 cells caused by transfection of shRNA-expressing pDNA. (A–C) Representative dot plots of the flow cytometric quantification of intact, apoptotic and necrotic cells. B16-BL6/dual Luc seeded on 6-well culture plates (at a density of 1×10^5 cells/well) were transfected with piGENE-hU6 (A), pshβ-catenin (B) or pshHIF1α (C). After 3 days incubation from the initiation of transfection, cells were processed and stained with annexin-FITC and PI as indicated in M&M. Live cells (annexin-FITC and PI double negative) occupy the lower left quadrant, early apoptotic cells (annexin-FITC positive and PI negative) occupy the lower right quadrant and late apoptotic or necrotic cells (annexin-FITC and PI double positive) occupy the upper right quadrant. (D) Percentage of viable, early apoptotic and late apoptotic or necrotic cells after transfection of shRNA-expressing pDNA, as calculated from the dot plots as in panel (A–C). The results are expressed as the mean±S.D. ($n=3$). *$P<0.05$ for Student's t-test versus control group.

was roughly estimated as the total number of apoptotic and necrotic cells, was about 20% of the total cells in the case of pshβ-catenin, 15% in the case of pshHIF1α and 10% in the case of control pDNA.

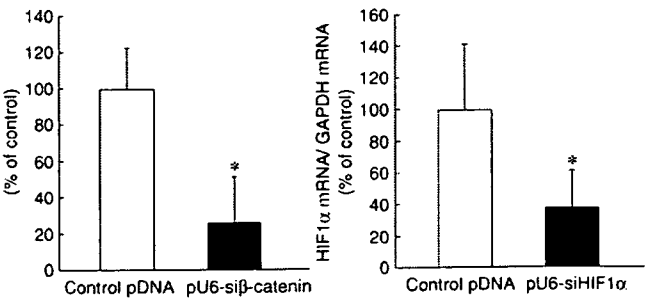

Fig. 4. Reduction of mRNA expression in primary tumor tissue by intratumoral injection of shRNA-expressing pDNA followed by electroporation. Mice received an intratumoral injection of piGENE-hU6 or shRNA-expressing pDNA (30 μg), followed by electroporation. Amounts of mRNA in tumor tissue were determined 24 h after administration. The results are expressed as the mean±S.D. ($n=4$). *$P<0.05$ for Student's t-test versus control group.

3.4. Reduction of mRNA and growth inhibition of subcutaneous tumor tissue of B16-BL6/dual Luc by intratumoral injection of pshβ-catenin or pshHIF1α

Fig. 4 shows the amount of β-catenin and HIF1α mRNA in B16 tumor tissue in mice 24 h after intratumoral injection of pshβ-catenin or pshHIF1α followed by electroporation. A single injection of each shRNA-expressing pDNA reduced the amount of the corresponding target mRNA in the tumor tissue. The mRNA level of β-catenin and HIF1α was reduced to 25 and 35% of the control value, respectively, demonstrating that intratumoral injection of shRNA-expressing pDNA can efficiently suppress the corresponding target gene expression in tumor tissue in mice.

To suppress the tumor growth in mice, tumor-bearing mice received intratumoral injection of shRNA-expressing pDNA followed by electroporation at day 7, 10 and 19 days after tumor inoculation. The injection of control pDNA followed by electroporation retarded the growth of tumor tissue compared with the no treatment group (data not shown). Intratumoral delivery of pshβ-catenin or pshHIF1α significantly reduced the growth of the tumor tissue compared with the delivery of control pDNA (Fig. 5A); the tumor volume was significantly suppressed by intratumoral delivery of pshβ-catenin or pshHIF1α 18 or 15 days after initiation of the therapeutic treatment, respectively. Tumor growth was suppressed in all mice treated with pshβ-catenin or pshHIF1α, and the tumor regressed markedly in two and one out of the four mice treated with pshβ-catenin or pshHIF1α, respectively, as shown in Fig. 5B–D.

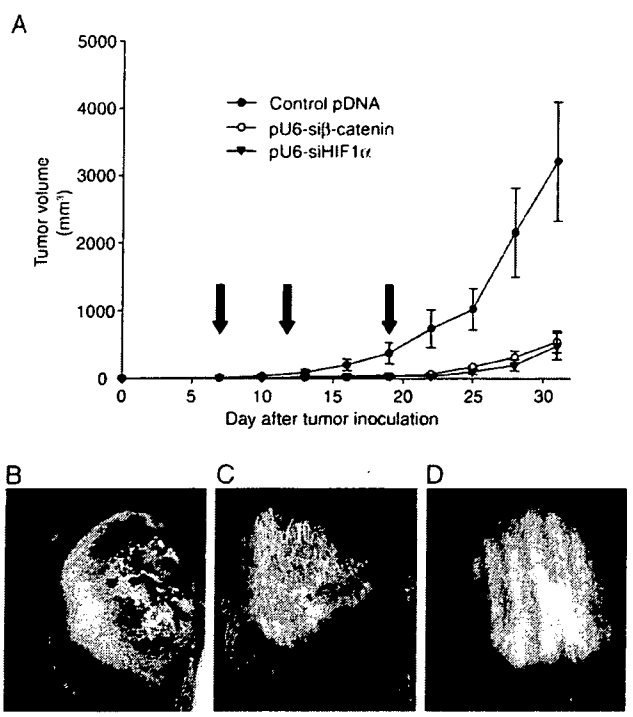

Fig. 5. Effects of intratumoral delivery of shRNA-expressing pDNAs on the growth of primary tumor tissue. (A) Mice received an intratumoral injection of 30 μg piGENE-hU6 or shRNA-expressing pDNAs followed by electroporation. shRNA-expressing pDNAs were administrated at day 7, 10 and 19 after tumor inoculation. Arrows indicate the timing of pDNA administration. The results are expressed as the mean±S.E.M. ($n=4$). *$P<0.05$ for Student's t-test versus control group. (B–D) Photographic image of tumor tissue of mice who received an intratumoral injection of piGENE-hU6 (B), pshβ-catenin (C) or pshHIF1α (D) at 18 days after initiation of therapeutic treatment.

4. Discussion

When B16 cells were transfected with pDNA expressing enhanced green fluorescent protein (EGFP) in vitro, a flow cytometric analysis demonstrated that about 80% of cells were EGFP positive at 24 h after transfection (unpublished data). Therefore, pDNA expressing shRNA can also be delivered to about 80% of cells in the transfection condition used, because the two plasmids are not quite different in size (3 kb for pDNA expressing shRNA and 4 kb for pDNA expressing EGFP). Transfection of pshβ-catenin and pshHIF1α was effective in suppressing corresponding target mRNA expression to about 20 or 25% of control value, respectively. Reduction in the mRNA expression of β-catenin or HIF1α was associated with a reduced number of viable cells. There are two different mechanisms governing the reduction in the proliferation of B16 tumor cells by the suppression of β-catenin or HIF1α expression: one is a reduced proliferation rate of B16 cells [21,22], and the other is an increased number of dead cells. To investigate whether the transfection of pshβ-catenin or pshHIF1α increases the number of dead cells, B16 cells were double-stained with annexin V conjugated with fluorescein and PI, and analyzed by flow cytometry to determine the ratio of dead cells to total cells. To analyze the growth and death rate of the transfected B16 cells, we assumed that cells proliferate and die according to first-order rate processes. The death rates of cells were calculated based on the data shown in Fig. 3D. To calculate the proliferation rates, the time course of the viable cell number after transfection was evaluated by simultaneously performing an MTT assay (data not shown). The calculated proliferation rates were 0.485 (control pDNA), 0.270 (pshβ-catenin) and 0.412 (pshiHIF1α), and the death rates of the cells were 0.0286 (control pDNA), 0.0948 (pshβ-catenin) and 0.0621 (pshHIF1α). These results suggest that both the increase in cell death and the decrease in cell proliferation rate contribute to the decrease in the number of B16 cells caused by the transfection of pshβ-catenin and pshHIF1α.

We have reported that electroporation significantly (about 10-fold) increases transgene expression in tumor tissues after intratumoral injection of pDNA expressing firefly luciferase [19]. Electroporation was also effective in suppressing target gene expression after intratumoral injection of shRNA-expressing pDNA. Intratumoral injection of shRNA-expressing pDNA suppressed target gene (firefly luciferase) expression to about 30% of the control value when combined with electroporation [19], but to about 80% without electroporation (unpublished data). Therefore, the delivery efficiency of shRNA-expressing pDNA can also be significantly increased by electroporation. An intratumoral injection of pshβ-catenin or pshHIF1α followed by electroporation successfully suppressed the corresponding target gene expression to the level below

30% of the control. Moreover, intratumoral delivery of pshβ-catenin or pshHIF1α also retarded in vivo tumor growth although the mRNA expression was not completely suppressed. Intratumoral injection of shRNA-expressing pDNAs followed by electroporation reduced target gene expression to about 30% of the control values, and the intensity of inhibitory effect was comparable with that of in vitro transfection, in which about 80% of cells receive plasmid DNA as mentioned above. Therefore, these results suggest that about 80% of the tumor cells receive the shRNA-expressing pDNA injected intratumorally, and that the delivery efficiency is enough to suppress tumor growth. Large tumor tissues with a diameter of over 6 mm were less sensitive to the same treatment than small ones of 2–3 mm in diameter (data not shown), suggesting the importance of the delivery efficiency of the shRNA-expressing pDNA. A combination with other therapeutic treatments, such as enhancing host immune response to tumor cells, could be an effective approach to further suppressing tumor growth.

5. Conclusion

We found that the silencing of β-catenin or HIF1α is effective in reducing the proliferation of melanoma cells. The delivery of pshβ-catenin or pshHIF1α to intradermal tumor tissues suppressed the corresponding mRNA expression and the growth of tumor tissue. These results indicate that strategies targeting β-catenin or HIF1α, including the use of RNAi, may be of use in the future treatment of cancer.

Acknowledgements

This work was supported in part by a Grant-in-Aid for Scientific Research from the Ministry of Education, Culture, Sports, Science and Technology, Japan and by a Health and Labor Sciences Research Grants from the Ministry of Health, Labor and Welfare of Japan.

References

[1] P.D. Zamore, T. Tuschl, P.A. Sharp, D.P. Bartel, RNAi: double-stranded RNA directs the ATP-dependent cleavage of mRNA at 21 to 23 nucleotide intervals, Cell 101 (1) (2000) 25–33.
[2] T. Tuschl, P.D. Zamore, R. Lehmann, D.P. Bartel, P.A. Sharp, Targeted mRNA degradation by double-stranded RNA in vitro, Genes Dev. 13 (24) (1999) 3191–3197.
[3] S.M. Hammond, E. Bernstein, D. Beach, G.J. Hannon, An RNA-directed nuclease mediates post-transcriptional gene silencing in *Drosophila* cells, Nature 404 (6775) (2000) 293–296.
[4] N. Kobayashi, Y. Matsui, A. Kawase, K. Hirata, M. Miyagishi, K. Taira, M. Nishikawa, Y. Takakura, Vector-based in vivo RNA interference: dose- and time-dependent suppression of transgene expression, J. Pharmacol. Exp. Ther. 308 (2) (2004) 688–693.
[5] Y. Matsui, N. Kobayashi, M. Nishikawa, Y. Takakura, Sequence-specific suppression of mdr1a/1b expression in mice via RNA interference, Pharm. Res. 22 (12) (2005) 2091–2098.
[6] S.M. Elbashir, J. Harborth, W. Lendeckel, A. Yalcin, K. Weber, T. Tuschl, Duplexes of 21-nucleotide RNAs mediate RNA interference in cultured mammalian cells, Nature 411 (6836) (2001) 494–498.
[7] N.J. Caplen, S. Parrish, F. Imani, A. Fire, R.A. Morgan, Specific inhibition of gene expression by small double-stranded RNAs in invertebrate and vertebrate systems, Proc. Natl. Acad. Sci. U. S. A. 98 (17) (2001) 9742–9747 Electronic publication 2001 Jul 31.
[8] O. Milhavet, D.S. Gary, M.P. Mattson, RNA interference in biology and medicine, Pharmacol. Rev. 55 (4) (2003) 629–648.
[9] H. Gong, C.M. Liu, D.P. Liu, C.C. Liang, The role of small RNAs in human diseases: potential troublemaker and therapeutic tools, Med. Res. Rev. 25 (3) (2005) 361–381.
[10] P.D. Rye, T. Stigbrand, Interfering with cancer: a brief outline of advances in RNA interference in oncology, Tumour Biol. 25 (5–6) (2004) 329–336.
[11] M. Izquierdo, Short interfering RNAs as a tool for cancer gene therapy, Cancer Gene Ther. 12 (3) (2005) 217–227.
[12] J.R. Bertrand, M. Pottier, A. Vekris, P. Opolon, A. Maksimenko, C. Malvy, Comparison of antisense oligonucleotides and siRNAs in cell culture and in vivo, Biochem. Biophys. Res. Commun. 296 (4) (2002) 1000–1004.
[13] R. Kretschmer-Kazemi Far, G. Sczakiel, The activity of siRNA in mammalian cells is related to structural target accessibility: a comparison with antisense oligonucleotides, Nucleic Acids Res. 31 (15) (2003) 4417–4424.
[14] A. Grunweller, E. Wyszko, B. Bieber, R. Jahnel, V.A. Erdmann, J. Kurreck, Comparison of different antisense strategies in mammalian cells using locked nucleic acids, 2′-*O*-methyl RNA, phosphorothioates and small interfering RNA, Nucleic Acids Res. 31 (12) (2003) 3185–3193.
[15] M. Miyagishi, M. Hayashi, K. Taira, Comparison of the suppressive effects of antisense oligonucleotides and siRNAs directed against the same targets in mammalian cells, Antisense Nucleic Acid Drug Dev. 13 (1) (2003) 1–7.
[16] Y. Zeng, B.R. Cullen, RNA interference in human cells is restricted to the cytoplasm, RNA 8 (7) (2002) 855–860.
[17] M. Stevenson, Therapeutic potential of RNA interference, N. Engl. J. Med. 351 (17) (2004) 1772–1777.
[18] L. Zender, S. Kubicka, SiRNA based strategies for inhibition of apoptotic pathways in vivo—analytical and therapeutic implications, Apoptosis 9 (1) (2004) 51–54.
[19] Y. Takahashi, M. Nishikawa, N. Kobayashi, Y. Takakura, Gene silencing in primary and metastatic tumors by small interfering RNA delivery in mice: quantitative analysis using melanoma cells expressing firefly and sea pansy luciferases, J. Control. Release 105 (3) (2005) 332–343.
[20] W.J. Nelson, R. Nusse, Convergence of Wnt, beta-catenin, and cadherin pathways, Science 303 (5663) (2004) 1483–1487.
[21] U.N. Verma, R.M. Surabhi, A. Schmaltieg, C. Becerra, R.B. Gaynor, Small interfering RNAs directed against beta-catenin inhibit the in vitro and in vivo growth of colon cancer cells, Clin. Cancer Res. 9 (4) (2003) 1291–1300.
[22] G.L. Semenza, Targeting HIF-1 for cancer therapy, Nat. Rev., Cancer 3 (10) (2003) 721–732.
[23] X. Sun, J.R. Kanwar, E. Leung, K. Lehnert, D. Wang, G.W. Krissansen, Gene transfer of antisense hypoxia inducible factor-1 alpha enhances the therapeutic efficacy of cancer immunotherapy, Gene Ther. 8 (8) (2001) 638–645.
[24] L. Li, X. Lin, M. Staver, A. Shoemaker, D. Semizarov, S.W. Fesik, Y. Shen, Evaluating hypoxia-inducible factor-1alpha as a cancer therapeutic target via inducible RNA interference in vivo, Cancer Res. 65 (16) (2005) 7249–7258.
[25] R. Supino, MTT assays, Methods Mol. Biol. 43 (1995) 137–149.

Available online at www.sciencedirect.com
SCIENCE DIRECT
Vaccine 24 (2006) 5535–5545
Vaccine
www.elsevier.com/locate/vaccine

Enhanced antigen-specific antibody production following polyplex-based DNA vaccination via the intradermal route in mice

Atsushi Kawase, Keiko Isaji, Ayumi Yamaoka, Naoki Kobayashi, Makiya Nishikawa, Yoshinobu Takakura *

Department of Biopharmaceutics and Drug Metabolism, Graduate School of Pharmaceutical Sciences, Kyoto University, Sakyo-ku, Kyoto 606-8501, Japan

Received 16 June 2005; received in revised form 24 April 2006; accepted 25 April 2006
Available online 5 May 2006

Abstract

DNA vaccination is an attractive approach with various advantages over conventional vaccination. The present study was undertaken to examine whether polyplex-based DNA vaccination could be used to modulate immune responses by plasmid DNA (pDNA). Methylated bovine serum albumin (mBSA) was used as a model of a cationic macromolecular carrier of pDNA encoding obalbumin (OVA) and the effects of polyplex formation of pDNA with mBSA on the antigen-specific immune responses were examined. Anti-OVA IgG antibody production was significantly increased following intradermal immunization with the polyplex compared with naked pDNA, although the induction of cytotoxic T lymphocyte activity was lowered by polyplex formation. We also demonstrated that the disposition and gene expression of pDNA following intradermal injection could be manipulated by polyplex formation. Intriguingly, we also found that the migration of dendritic cells to the injected site could be induced by polyplex formation probably due to a high level of tumor necrosis factor α production from the keratinocytes treated with mBSA/pDNA complexeses. Thus, the present study has demonstrated that the immune responses could be biased towards a Th2-type response by polyplex-based DNA vaccination through manipulation of not only pDNA disposition but also dendritic cell migration.

Keywords: DNA vaccine; Polyplex; Dendritic cell

1. Introduction

DNA vaccination is the approach that can induce both humoral and cellular immune responses against various diseases by injection of plasmid DNA (pDNA) encoding antigen [1,2]. These responses include protective neutralizing antibodies and antigen-specific cytotoxic T lymphocytes (CTL). Professional antigen presenting cells, such as dendritic cells (DC), most likely play a key role in initiating primary immune responses after DNA vaccination [3,4]. The induction of antigen-specific immune responses occurs through the presentation of appropriate peptides in the context of major histocompatibility polyplex (MHC) molecules on DC. In general, DC appear to play at least three distinct roles in genetic immunization: (1) MHC class II-restricted presentation of antigens that are secreted by the neighboring, transfected somatic cells; (2) MHC class I-restricted, "cross-presentation" of antigens that are released by the transfected somatic cells; and (3) direct presentation of antigens that are produced endogenously in the transfected DC themselves. We hypothesized that antigen-specific immune responses depending on these processes could be modulated by manipulation of the profiles of local disposition of pDNA and subsequent protein expression following immunization by polyplexation with cationic macromolecules.

In this study, we investigated the effect of polyplex formation on the antigen-specific immune responses induced by DNA vaccination to test this hypothesis. We prepared a pDNA/cationic polymer polyplex, i.e., polyplex, using

* Corresponding author. Tel.: +81 75 753 4615; fax: +81 75 753 4614.
E-mail address: takakura@pharm.kyoto-u.ac.jp (Y. Takakura).

0264-410X/$ – see front matter © 2006 Elsevier Ltd. All rights reserved.
doi:10.1016/j.vaccine.2006.04.056

pDNA encoding ovalbumin (OVA) expressing plasmid [5] and methylated bovine serum albumin (mBSA), which has been shown to act as an adjuvant [6,7].

We performed the immunization via the intradermal route because skin contains numerous, readily accessible cutaneous DC [epidermal Langerhans cell (LC) and dermal DC] and the keratinocytes (KC) which account for 90–95% of the cells in the epidermis are known to produce proinflammatory cytokines, such as interleukin (IL)-1, tumor necrosis factor α (TNF-α) and granulocyte-macrophage colony stimulating factor (GM-CSF) in response to allergens, infection, or injury [8]. These cytokines can promote DC and LC maturation, and are taken up from the blood and migrate to regional lymph nodes where antigenic peptides presented to naïve T cell and primary T cell responses are triggered [9,10].

The present study suggests that the anti-OVA IgG antibody response, the Th2-type response, is enhanced by polyplex formation. We have also shown that polyplex formation significantly affects the local disposition and subsequent transgene expression of pDNA following intradermal injection. Intriguingly, we have also found that polyplex administration induces DC accumulation in the injection site. It was found that the disposition of pDNA and DC in treated skins could be modified by polyplex formation. Thus, the present study demonstrates that the immune responses can be modulated by polyplex-based DNA vaccination through manipulation of not only pDNA disposition but also dendritic cell migration.

2. Materials and methods

2.1. Mice

Five- to six-week old female ddY or C57BL/6 (immunization experiment) mice were purchased from Japan SLC Co. (Shizuoka, Japan) and maintained under conventional housing conditions. Mice were anesthetized by inhalation of ether and euthanized by cervical dislocation.

2.2. Plasmid DNA

In the immune response experiments, we used pDNA encoding ovalbumin (OVA), pOVA, as a model antigen-expressing pDNA. pOVA was a kind gift from Dr. Shoshana Levy (Department of Medicine/Oncology, Stanford University Medical Center, Stanford USA). In the gene expression experiments, we used pLuc containing the firefly luciferase gene under the control of the CMV promoter. The pDNA was constructed by subcloning the *Hin*dIII/*Xba*I firefly luciferase cDNA fragment from pGL3-control vector into the polylinker of the pcDNA3 vector. In the confocal microscopic study, we used pGeneGrip™ (Rhodamine/GFP) (Gene Therapy Systems, San Diego, CA, USA) to observe co-localization of pDNA and transgene expression.

The pDNA amplified in the *DH5α* strain of *Escherichia coli* was extracted and purified using a QIAGEN Endofree™ Plasmid Giga Kit (QIAGEN GmbH, Hilden, Germany). The purity was checked by 1% agarose gel electrophoresis followed by ethidium bromide staining. The pDNA concentration was measured by UV absorption at 260 nm. To minimize activation by contaminated lipopolysaccharide (LPS) for in vitro experiments (Fig. 10), DNA samples were purified extensively with Triton X-114 (Nacalai Tesque, Kyoto, Japan), a non-ionic detergent [11,12]. DNA samples were purified by extraction with phenol: chloroform: isoamyl alcohol (25:24:1) and ethanol precipitation. DNA (10 mg) was diluted with 20 mL pyrogen-free water, and then 200 μL Triton X-114 was added followed by mixing. The solution was placed on ice for 15 min and incubated for 15 min at 55 °C. Subsequently, the solution was centrifuged for 20 min at 25 °C, 600 × *g*. The upper phase was transferred to a new tube, 200 μL Triton X-114 was added, and the previous steps were repeated three or more times. The activity of LPS was measured by limulus amebocyte lysate (LAL) assay using the Limulus F Single Test kit (Wako, Tokyo, Japan). After Triton X-114 extraction, the endotoxin levels of DNA samples could no longer be determined by LAL assay; i.e., 1 μg/mL DNA contained less than 0.001 EU/mL. Without extraction of endotoxin by Triton X-114, 100 μg/mL naked pDNA, which contains 1–5 EU/mL endotoxin, could release 521 ± 73 pg/mL TNF-α over 24 h.

2.3. Preparation of mBSA/pDNA complexeses

mBSA was synthesized from BSA (96–99%, standard grade) (Sigma, St. Louis, MO, USA) according to an earlier report [13]. Briefly, BSA was mixed with absolute methyl alcohol under acidic conditions (hydrochloric acid). In this process, the carboxyl group of the acidic amino acids in BSA was esterified and BSA was converted to a cationic macromolecule; the yield from this reaction was virtually 100%. mBSA/pDNA complexeses were prepared by adding various amounts of mBSA to pDNA to give different charge ratios (+/−). The final concentration of pDNA was adjusted to 0.1 μg/μL in 5% dextrose.

2.4. Immunization

Female C57BL/6 mice were injected intradermally in the dorsal region with 20, 40 (Fig. 2) or 100 μg (Figs. 2 and 4) pOVA or pOVA polyplexed with mBSA at biweekly intervals or only a single application was given. Control animals received 100 μg OVA protein (Sigma, St. Louis, MO, USA) emulsified in complete Freund's adjuvant (CFA) [14] (ICN Biomedicals Inc. Aurora, OH, USA) intraperitoneally.

2.5. Determination of total IgG and IgG1 or IgG2a subclass of anti-OVA antibodies titers by enzyme-linked immunosorbent assay

Serum samples were collected from the tail vein of mice to determine anti-OVA IgG, IgG1 and IgG2a antibodies titers.

The levels of antibodies were measured by enzyme linked immunosorbent assay (ELISA). OVA (1 mg/mL) in carbonate/bicarbonate buffer (0.1 M, pH 9.6) was distributed to each well of 96-well flat-bottom polystyrene plates (100 μL/well). Following overnight incubation at 4 °C, wells were blocked with 5% BSA-containing Tween-20 phosphate buffered saline (T-PBS) [0.5% (w/w) Tween-20 (ICN Biomedicals Inc. Aurora, OH, USA) in PBS] for 30 min at 37 °C. After the wells were washed three times with T-PBS, serially diluted 100 μL serum samples were added to the wells. After 2 h incubation at 37 °C, the wells were washed five times with T-PBS and 100 μL anti-IgG, IgG1 or IgG2a-HRP conjugate (Sigma, St. Louis, MO, USA), diluted 2000:1 with 5% BSA-containing T-PBS, was add to each well. After a 2 h incubation, each well was washed with T-PBS and then 200 μL freshly prepared *o*-phenylenediamine dihydrochloride (Wako, Tokyo, Japan) solution in phosphate-citrate buffer (0.05 M, pH 5.0) was added to each well. After a 30 min incubation, 50 μL 10% H_2SO_4 was added and then the absorbance was measured at 490 nm. Serum total IgG, IgG1 and IgG2a titers were estimated by the dilution ratio at which an absorbance value of 0.1 was obtained.

2.6. CTL assay

In the CTL assay, we used EL4 and E.G7 (EL4 expressing OVA) as target cells. EL4 cells were cultured in Dulbecco's modified Eagle medium (Nissui Pharmaceutical, Tokyo, Japan) supplemented with 10% heat-inactivated fetal bovine serum (FBS) (Thermo Trace, Melbourne, Australia), 2 mM L-glutamine and antibiotics. E.G7 cells were cultured in RPMI 1640 medium supplemented with 10% heat-inactivated FBS, 50 μM 2-mercaptoethanol (2-ME) (Sigma, St. Louis, MO, USA), 2 mM L-glutamine, glucose, sodium pyruvate, HEPES (Nacalai Tesque, Kyoto, Japan) and G418. Immunization was performed three times at biweekly intervals. One week after the last immunization, spleen cells were isolated from the immunized mice and restimulated in vitro for 5 days with mitomycin C-treated E.G7. Target cells were labeled with ^{51}Cr by incubating with $Na_2{}^{51}CrO_4$ (Daiichi Radioisotope Labs, Tokyo, Japan) in culture medium for 45 min at 37 °C. After washing, 2×10^4 of the ^{51}Cr-labeled target cells and serially diluted spleen cells were coincubated in 200 μL culture medium for 4 h at 37 °C. Spontaneous release of ^{51}Cr without effector cells and maximal release in the presence of 1% NP40 were also evaluated. Cells were centrifuged (1500 rpm) for 5 min, and 100 μL of each supernatant was collected for radioactivity measurements. The cytolytic activity of CTL was calculated as [15]:

$$\%\ \text{killing} = 100 \times \frac{(\text{observed release} - \text{spontaneous release})}{(\text{maximal release} - \text{spontaneous release})}.$$

2.7. Determination of cytokine production from spleen cells and proliferation of antigen-specific T cells

At 4 weeks after the final immunization, spleen cells isolated from immunized mice were cocultured with OVA protein in RPMI 1640 medium supplemented with 10% heat-inactivated fetal FBS, 10 mM HEPES, 1 mM sodium pyruvate, 0.1 mM non-essential amino acids, 2 mM L-glutamine and 50 mM 2-ME at 37 °C for 3 days. The levels of cytokines (IL-12, IL-10 and IL-4) released into the culture medium were measured by a suitable ELISA kit (ANALYZA mouse IL-12, IL-10 and IL-4, genzyme TECHNE, Minneapolis, MN, USA). The proliferation of antigen-specific T cells was determined by Alamar Blue assay (Alamar BioSciences, Sacramento, CA, USA), based on the bioreduction of a fluorogenic substrate.

2.8. In vivo reporter gene assay after intradermal administration

A 1.5 cm × 1.5 cm area of skin was removed from each mouse at 1 or 3 days after intradermal administration of naked pLuc or mBSA/pLuc polyplexes. Tissues were homogenized with lysis buffer [0.1 M Tris (Wako, Tokyo, Japan), 0.05% Triton X-100 (Nacalai Tesque, Kyoto, Japan), 2 mM EDTA (Wako, Tokyo, Japan), pH 7.8], and subjected to three cycles of freezing (−190 °C) and thawing (37 °C). The homogenates were centrifuged at 14,000 × *g* for 8 min at 4 °C. Ten μL supernatant was mixed with 100 μL luciferase assay buffer (Picagene, Toyo Ink, Tokyo, Japan) and the chemiluminescence produced was measured in a luminometer (Lumat LB 9507, EG & G Berthold, Bad Wildbad, Germany).

2.9. Confocal microscopic studies of localization of pDNA and expressed proteins

Mice (female ddY) were injected with 20 μg pGeneGrip™ (Rhodamine/GFP) intradermally. We could observe the disposition of both pDNA and expressed protein because this pDNA is rhodamine-labeled pDNA encoding GFP. At 1 or 24 h after injection, mice were euthanized and their skins were excised. Cryosections, 10 μm thick, were prepared using a cryostat (Jung Frigocut 3000E, Leica Microsystems AG, Wetzlar, Germany) and fixed in 10% neutral formalin. The sections were examined by confocal microscopy (MRC-1024, BioRad, Hercules, CA, USA).

2.10. Flow cytometric analysis of the presence of $CD11c^+$ cells in skin

In this experiment, 20 μg pOVA or pOVA polyplexed with mBSA (8:1) was injected into the skin. After 6 h, the skin was excised and treated with 1% trypsin (Invitrogen Corp., Carlsbad, CA USA) for 1 h at 37 °C. Following removal of the epidermis from the dermis, it was treated in 0.025%

DNase I (Sigma, St. Louis, MO, USA) for 20 min. The cells of the treated epidermis were extruded using a sterilization stick and washed three times in RPMI 1640. After the supernatant was removed, the obtained KC were resuspended in 150 μL PBS containing 0.5% BSA per 10^8 total cells. The cell suspension was mixed with 50 μL (2 μg) fluorescein isothiocyanate (FITC)-conjugated anti-mouse CD11c antibody (BD Biosciences, USA) and incubated for 15 min at 4 °C. After adding 10 mL PBS, the supernatant was removed and the cells were resuspended in 500 μL PBS. Flow cytometric analysis to detect the presence of $CD11c^+$ cells in the skin was performed using a FACSCalibur cytometer (Becton Dickenson, SanJose, CA, USA) and cellquest software (Becton Dickenson, SanJose, CA, USA). We confirmed that there was a significant difference between the histograms of pOVA and that of mBSA/pOVA (8:1) by CellQuest software (Becton Dickinson).

2.11. Accumulation of $CD11c^+$ cells in treated skins of immunized mice

Injections of 20 μg of pOVA or pOVA polyplexed with mBSA (8:1) were made into the skin and, after 6 h, the skin cells were isolated. We used murine bone marrow-derived dendritic cells (BMDC) after differentiation of cells isolated from murine bone marrow. After the bone marrow was flushed out from the bones of the murine hind legs, the cells were cultured in RPMI 1640 medium supplemented with 10% FBS and 1000 U/mL rGM-CSF. After 4 to 5 days incubation at 37 °C in 5% CO_2–95% air, cells were collected and centrifuged at 200 × *g* for 10 min. After the supernatant was removed, the cells were resuspended in 400 μL of PBS containing 0.5% BSA per 10^8 total cells. The cell suspension was mixed with 100 μL mouse CD11c MicroBeads (Miltenyi Biotec, Germany) and incubated for 15 min at 4 °C. CD11c is one of the differentiation antigens of DC. Cells were washed, centrifuged at 200 × *g* for 10 min, and resuspended in 500 μL PBS containing 0.5% BSA. Then, magnetic separation with magnetic cell sorting (MACS) (autoMACS, Miltenyi Biotec, Germany) was carried out to isolate DC, by selecting CD11c-positive (+) cells from all the cultured cells. We confirmed that the recovery efficacy of the $CD11c^+$ cells was not variable between preparations by preliminary experiments.

2.12. Determination of TNF-α release from cultured KC

KC isolated as described in the flow cytometric analysis were cultured with Keratinocyte-SFM (Invitrogen Corp., Carlsbad, CA USA) in 24-well plates. After washing three times with 0.5 mL Keratinocyte-SFM, 1.5 μg pOVA or pOVA polyplexed with mBSA (8:1) was transfected. After 18 h incubation, the supernatant was collected and the concentration of TNF-α was analyzed by ELISA (ANALYZA mouse TNF-α, genzyme TECHNE, Minneapolis, MN, USA).

2.13. Statistics

Significant differences between mean values of the levels of gene expression were estimated using the Student's paired *t*-test after ANOVA.

3. Results

3.1. Determination of total IgG and IgG1 or IgG2a subclass of anti-OVA antibodies titers

We investigated the effects of polyplex formation on the types of immune responses induced by DNA vaccination. Antigen-specific immune responses induced following DNA vaccination include CTL induction and antibody production. To examine whether the antigen-specific antibody production was affected by polyplex formation, we measured the

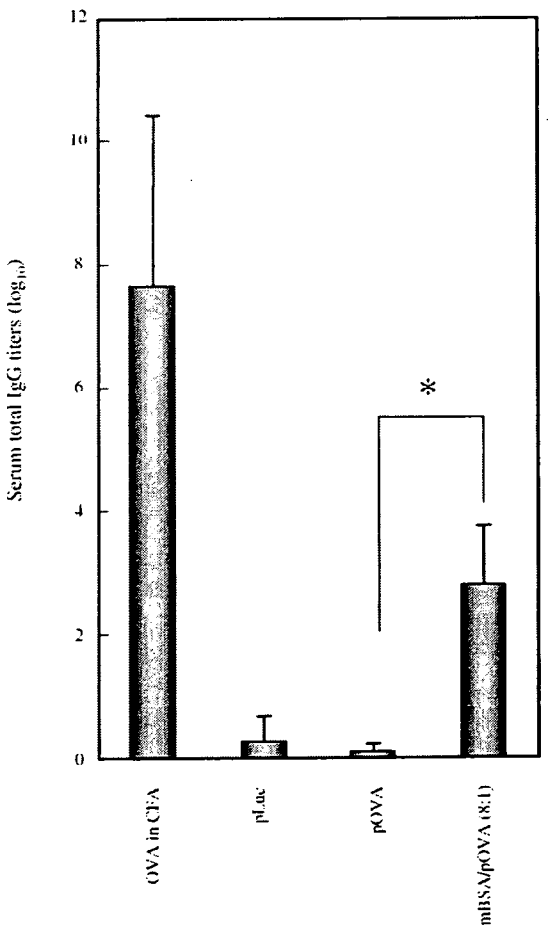

Fig. 1. Production of total anti-OVA IgG antibody at 6 weeks after single immunization of pOVA or mBSA/pOVA polyplexes (8:1) via the intradermal route. The serum samples from immunized mice were collected and the antibody titers were measured by ELISA. The results are expressed as mean ± S.D. of four mice. *Indicates a significant difference between the values of pOVA and mBSA/pOVA (8:1) ($p < 0.01$).

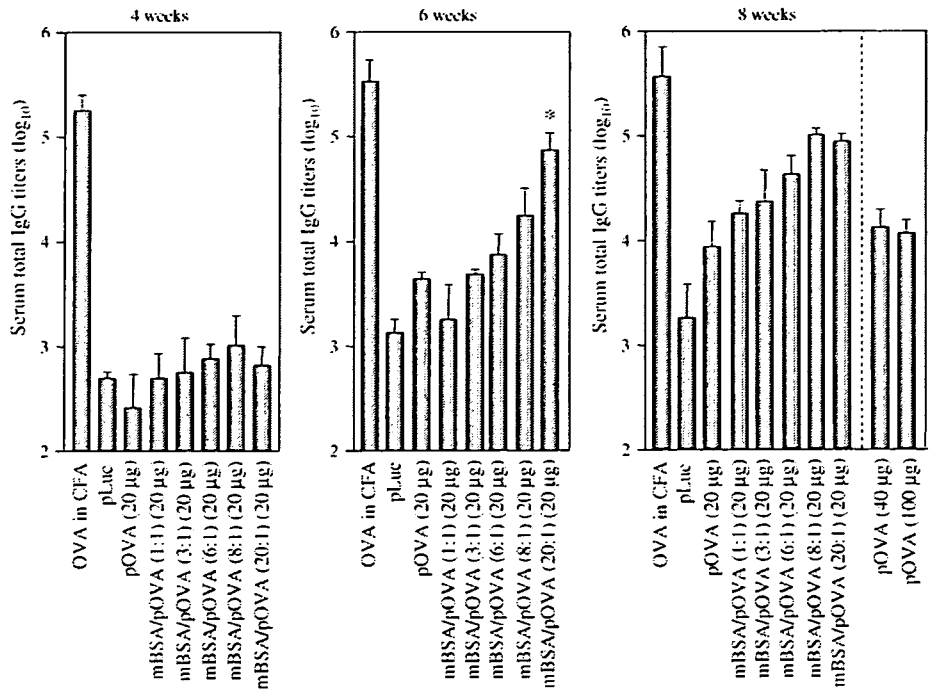

Fig. 2. Production of total anti-OVA IgG antibody after biweekly immunization of pOVA or mBSA/pOVA polyplexes via the intradermal route. The serum samples from immunized mice were collected and the antibody titers were measured by ELISA. The results are expressed as mean ± S.D. of four mice. *Indicates a significant difference between the values of pOVA and mBSA/pOVA (20:1) ($p < 0.01$).

amount of anti-OVA IgG antibodies in immunized mice. Fig. 1 shows the total anti-OVA IgG antibody level after a single immunization. A significantly increased level of total anti-OVA IgG antibody was obtained in mice immunized with mBSA/pOVA polyplexes (8:1), whereas little antibody response was detected in mice immunized with naked pOVA. We also examined the total IgG level following biweekly immunization with polyplexes with different charge ratios (Fig. 2). A marked increase in IgG titers was obtained by biweekly intradermal administration of mBSA/pOVA polyplexes, particularly at the higher charge ratios. In the mBSA/pOVA polyplexes (8:1) or (20:1), the levels of antibody were increased up to 4.0 or 15.7 times at 6 weeks and up to 11.5 or 11.0 times at 8 weeks, respectively, compared with that of naked pOVA. It was also found that the levels of IgG antibody production in mice treated with mBSA/pOVA polyplexes were higher than those in mice treated with higher doses (40 or 100 μg) of naked pOVA. These results show that the required dose of pDNA and the required number of immunizations to induce an antibody response can be reduced by polyplex formation. Further, we examined the subclass of anti-OVA IgG antibody to determine the type of promoted immune responses (Fig. 3). The levels of anti-OVA IgG2a antibody production were similar in mice treated with polyplexes and naked pDNA. On the other hand, a significant production of anti-OVA IgG1 antibody was detected in mice treated with mBSA/pOVA polyplexes but not in mice treated with naked pOVA at the same dose, indicating

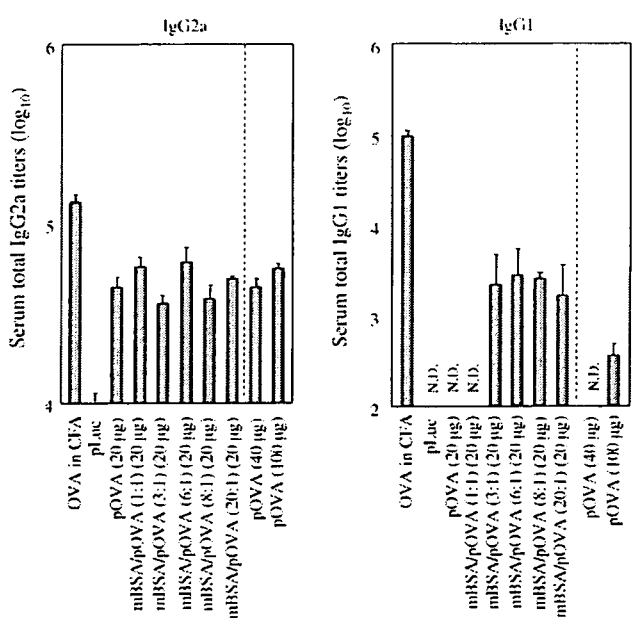

Fig. 3. Production of IgG1 or IgG2a subclasses of anti-OVA antibody at 8 weeks after biweekly immunization of pOVA or mBSA/pOVA polyplexes via the intradermal route. The serum samples from immunized mice were collected and the antibody titers were measured by ELISA. The results are expressed as mean ± S.D. of four mice.

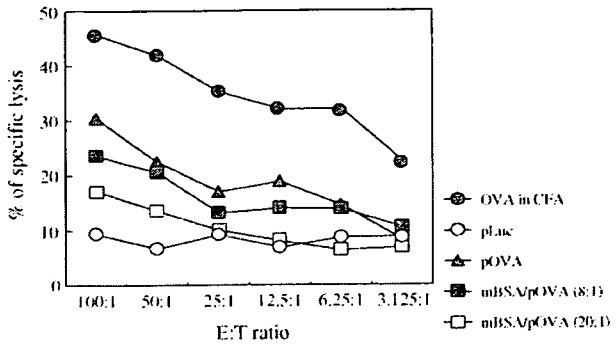

Fig. 4. Generation of OVA-specific CTL by immunization with pOVA or mBSA/pOVA polyplexes via the intradermal route. Mice were immunized four times with 100 μg pOVA or pOVA polyplexed with mBSA. Seven days after the last immunization, spleen cells were isolated and a standard ^{51}Cr-release assay was performed using the spleen cells cultured for 5 days.

that Th2-type immune responses are promoted by polyplex formation.

3.2. CTL assay

As the effect of polyplex-based DNA vaccination on antibody responses was demonstrated, we next examined whether this approach could affect the CTL response. In the experiment involving the CTL assay, we used mBSA/pOVA polyplexes (8:1) and (20:1) which showed an enhanced antibody response (Fig. 2). The activities of antigen-specific CTL response against E.G7 obtained by these polyplexes were slightly reduced compared with that obtained by naked pOVA (Fig. 4). We confirmed the antigen specificity by the minor degree of cell killing detected in EL4 (data not shown). The cpm values of spontaneous release and maximal release were 540.4 and 6568, respectively.

3.3. Determination of cytokine production from spleen cells and proliferation of antigen-specific T cells

To clarify the effect of polyplex-based DNA vaccination on immune responses, we investigated the responsiveness of spleen cells from immunized mice against OVA protein, although the analysis of sentinel lymph node also may provide additional information. We determined the levels of cytokine production from the spleen cells pulsed with OVA protein in Fig. 5A. The levels of IL-10 and IL-4 (Th2-type cytokines) released from spleen cells were increased by polyplex formation although the levels of IL-12 (Th1-type cytokine) scarcely changed. Fig. 5B shows that the proliferation of antigen-specific T cells was also promoted by polyplex formation, suggesting that the immune system was activated following polyplex-based DNA vaccination.

3.4. Reporter gene assay after intradermal administration

We demonstrated that the immune responses induced by DNA vaccination could be modulated by polyplex formation. We assumed that the gene expression and the disposition of pDNA following local injection were significantly altered by polyplex formation and these alterations would affect the immune responses. To examine whether the levels of trans-

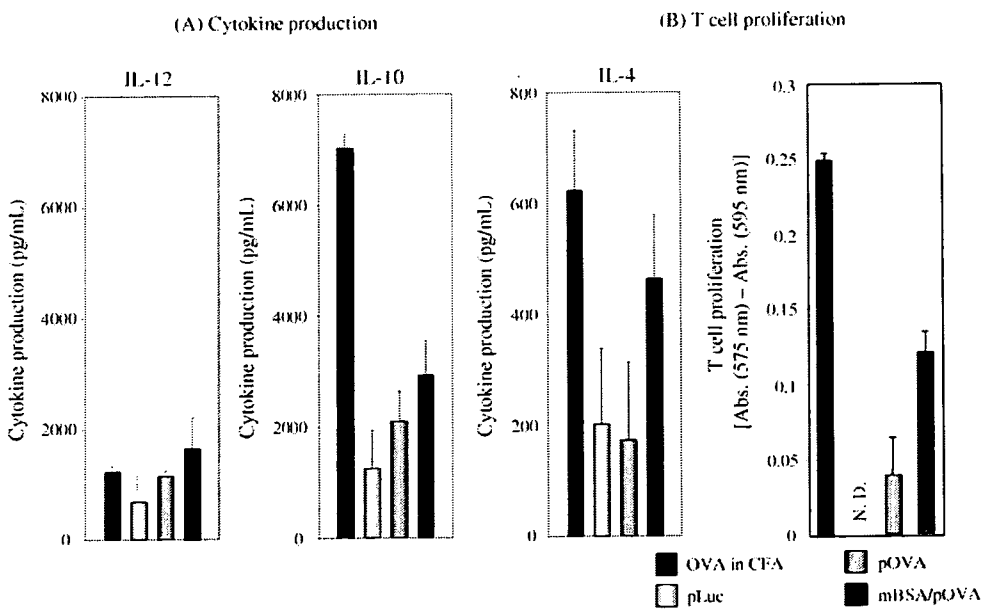

Fig. 5. (A) production of cytokines from spleen cells and (B) proliferation of antigen-specific T cells after immunization of pOVA or mBSA/pOVA polyplexes (A; 20:1, B; 6:1). (A) At 4 weeks after the final immunization, spleen cells isolated from immunized mice were co-cultured with OVA protein at 37 °C for 3 days. The levels of cytokines release into the culture medium were measured by ELISA. The results are expressed as mean ± S.E.M. of three wells. (B) The proliferation of antigen-specific T cells was determined by Alamar Blue assay. The results are expressed as mean ± S.D. of three wells.

gene expression were affected by polyplex formation, we carried out in vivo quantitalive gene expression experiments using pDNA encoding luciferase (pLuc). We measured the levels of gene expression in the skin at 1 or 3 days after administration (Fig. 6). Intradermal administration of naked pLuc resulted in a relatively high level of gene expression. A similar level of gene expression was obtained by intradermal administration of mBSA/pLuc polyplexes (1:1). On the other hand, the levels of gene expression were dramatically reduced in mBSA/pLuc polyplexes (3:1), (6:1), (8:1) and (20:1) depending on the mixing ratio, indicating that polyplex formation significantly reduced transgene expression at the injection site (Fig. 6).

3.5. Confocal microscopic studies of localization of pDNA and expressed protein

The disposition of pDNA and expressed proteins is important for the induction of immune responses. To investigate whether the localization of pDNA and expressed protein was affected by polyplex formation, we examined the tissue sections by confocal microscopy at 1 and 24 h following intradermal administration of pGeneGrip™ (Rhodamine/GFP) or mBSA/pGeneGrip™ polyplexes (8:1) which showed a high antibody response (Figs. 1 and 2) and a very low level of gene expression (Fig. 6). Red signals derived from naked rhodamine-labeled pDNA were observed in the dermis at 1 h (Fig. 7A and B). In the case of the mBSA/pGeneGrip™ polyplexes (8:1), we observed that a greater number of red signals remained in the vicinity of the injection site (Fig. 7B). This

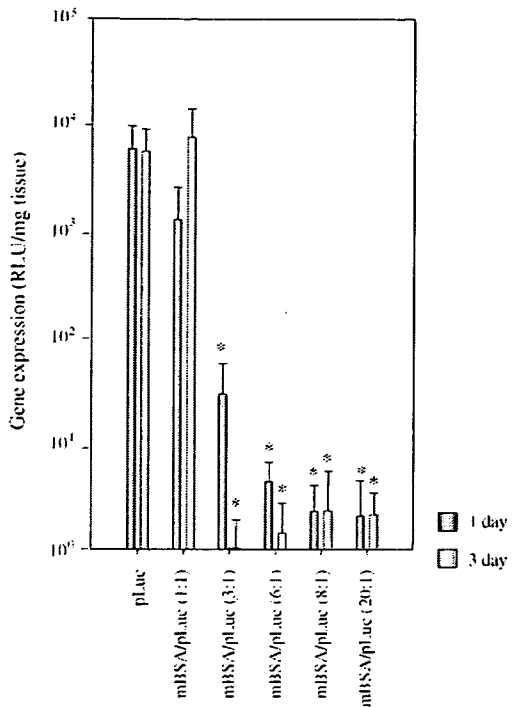

Fig. 6. Gene expression at 1 or 3 days after intradermal administration of pLuc or mBSA/pLuc at various charge ratios. The luciferase assay was performed on a 1.5 cm × 1.5 cm area of skin removed from each mouse. Four mice were used per group and the results are expressed as the mean ± S.D. *Indicates a significant difference ($p < 0.01$).

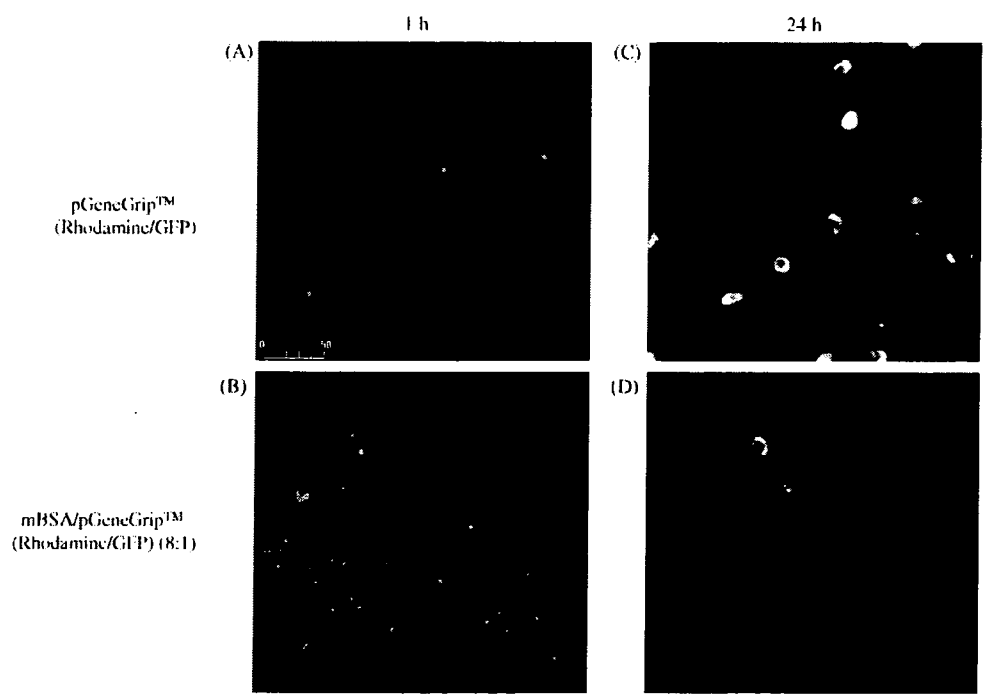

Fig. 7. Confocal microscopic images of a tissue section of mouse dorsal skin 1 or 24 h after intradermal administration of 20 μg pGeneGrip™ (rhodamine/GFP) (A) (×400) or pGeneGrip™ polyplexed with mBSA (3:1) (B) (×400).

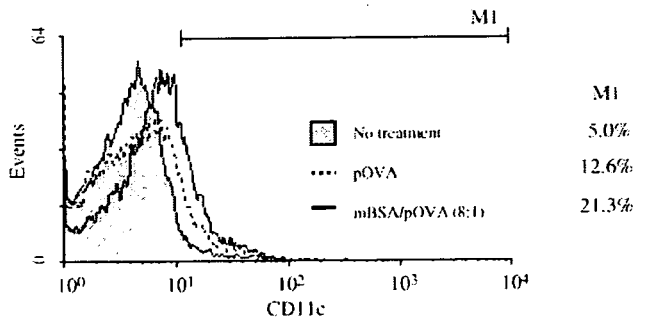

Fig. 8. Flow cytometric analysis of the presence of CD11c$^+$ cells in skin. Mice were given injections of 20 μg of pOVA or mBSA/pOVA polyplexes (8:1) into the skin. After 6 h, the isolated epidermis cells were treated with FITC-conjugated anti-mouse CD11c antibody and subjected flow cytometric analysis.

result suggests that the elimination of pDNA from the treated site was retarded by polyplex formation probably due to the electrostatic interaction with the tissue and the prevention of pDNA degradation there. At 24 h, green signals derived from GFP were observed in both images (Fig. 7C and D). A higher amount of GFP protein was observed in naked pGeneGrip^{TM} (Fig. 7C). This result shows that the level of gene expression at the injection skin was reduced by polyplex formation and this agrees with the results shown in Fig. 6.

3.6. Accumulation of CD11c$^+$ cells in treated skins of immunized mice

DC migration is one of the key events in the induction of immune responses. We speculated that polyplex formation might affect not only pDNA disposition/gene expression but also DC migration to the treated skin, which may be another factor modulating the immune responses. We investigated the effect of polyplex formation on the accumulation in the treated skin of endogenous DC after intradermal administration. Fig. 8 shows the results of the flow cytometric analysis. The ratio of CD11c$^+$ cells per 10,000 cells in the skin treated with mBSA/pOVA (8:1) was higher than that of the control or naked pOVA. We also measured the number of CD11c$^+$ cells in the treated skins using the MACS procedure (Fig. 9).

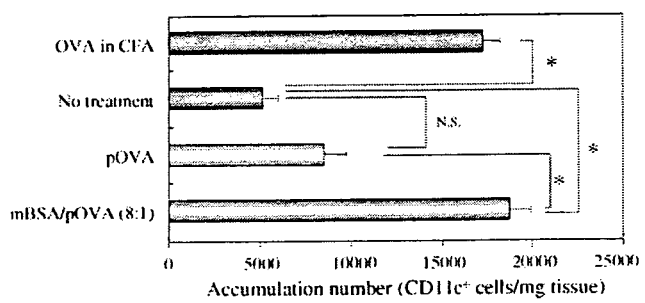

Fig. 9. Accumulation of CD11c$^+$ cells in the treated skin of immunized mice at 6 h after intradermal administration of pOVA or mBSA/pOVA polyplexes. *Indicates a significant difference ($p < 0.01$). N.S.; not significant.

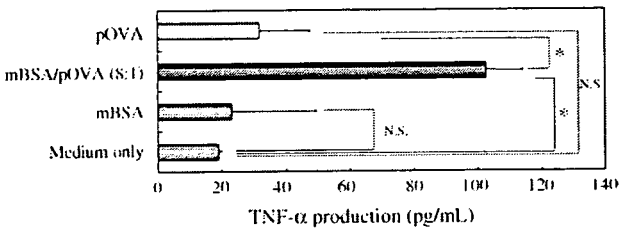

Fig. 10. Production of TNF-α from KC at 12 h after transfection of 5.0 μg pOVA, mBSA/pOVA polyplexes (8:1). The results are expressed as mean ± S.D. of six wells. *Indicates a significant difference ($p < 0.01$). N.S.; not significant.

In the case of naked pOVA, the number of CD11c$^+$ cells was not significantly increased compared with no treatment. The number of accumulated CD11c$^+$ cells was confirmed to increase significantly following injection of the polyplex. These results indicate that the number of DC in the treated skin was increased by polyplex formation, suggesting that mBSA/pDNA complexeses are efficiently taken up by these migrating DC.

3.7. Determination of TNF-α release from cultured KC

It is known that various cytokines, including TNF-α and IL-1β, are involved in DC migration. In particular, TNF-α mainly acts by producing accumulation of DC in the skin. We carried out an in vitro experiment using ketatinocytes (KC) in primary culture to examine whether TNF-α release occurs from KC in Fig. 10. pOVA or mBSA alone did not induce any significant level of TNF-α from the cultured KC. In contrast, mBSA/pOVA polyplexes (8:1) stimulated the KC to produce a significant amount of TNF-α. It is likely that this TNF-α production from KC is one of the important factors governing the induced accumulation of DC in treated skins in vivo.

4. Discussion

DNA vaccines produce both CTL induction and antibody production against encoded antigens. Each response also exerts a mutual action to control the balance of the immune responses [16,17]. To optimize immunotherapy, it is important to adjust the appropriate immune responses for various diseases. In this study, we investigated the effect of polyplex-based DNA vaccination on immune responses based on the consideration that the disposition and subsequent gene expression after local administration of pDNA are important factors determining the immune responses. Little information is available on polyplex-based DNA vaccination [18,19]. We used mBSA as a model cationic macromolecule and prepared the corresponding polyplex.

The present study has demonstrated that the anti-OVA IgG antibody responses are significantly increased in mice

immunized with the polyplex (Figs. 1 and 2), indicating that mBSA is a useful carrier for production of antibody. On the other hand, CTL activity induced by the polyplex is reduced (Fig. 4). It has been also shown that productions of IgG1 subclass of anti-OVA antibody (Fig. 3) and IL-10 and IL-4 from the spleen cells (Fig. 5) are increased. Our results suggest that the antigen-specific antibody production by polyplex immunization was increased under Th2 cytokine environment. Recent report has also demonstrated that $CD8^+$ and $CD8^-$ DC subsets could induce CTL response with higher Th2 cytokines [20].

The present study also demonstrated that the levels of gene expression in the injection site were dramatically reduced compared with naked pDNA (Figs. 6 and 7). This observation was somewhat unexpected because antibody production was increased. We previously reported the effects of complex formation on the disposition and gene expression after intramuscular injection [21]. Similar effects would be expected in the case of intradermal injection. We consider that the increased antibody production would be ascribed to (1) improvement of retention of pDNA in the treated skins and disposition of pDNA in the regional lymph nodes, (2) elevation of the accumulation of DC to the treated skins, (3) prevention of pDNA from degradation.

Our previous in vitro study demonstrated that pDNA complexed with mBSA enhanced transfection efficiency in DC2.4 cells, murine DC cell line [21]. However, in vivo pDNA delivery by cationic complex would lead to restricted distribution of pDNA in the skin compared with naked pDNA that could widely distribute throughout the skin and show a higher gene expression in keratinocytes, but not in DC. We speculated that the levels of gene expression in DC were increased by complex formation in not only in vitro but also in vivo condition. However, the levels of gene expression of DC in the skin did not contribute to the overall level of gene expression in the entire skin because the number of DC in skin is very low. Therefore, overall gene expression in the injection site in vivo was significantly decreased compared with naked pDNA (Figs. 6 and 7).

Increased antibody production might be explained, at least in part, by the interesting phenomenon that significant accumulation of DC in the treated skin occurred following polyplex injection (Figs. 8 and 9). In vitro experiments using cultured KC suggest that TNF-α production from KC upon stimulation with the polyplex is one of the important factors governing the induction of DC accumulation. In addition to the prolonged retention of the polyplex at the injection site (Fig. 7), this DC accumulation would be advantageous for direct interaction of pDNA with DC. We speculated that the efficiency of pDNA uptake by DC was improved at the injection site treated with mBSA/pDNA complexeses. In our previous study, we showed that the levels of in vitro gene expression and cytokine induction in DC2.4 cells were increased by polyplex formation [21]. Although attention has to be paid to the interpretation of the data obtained under in vivo and in vitro conditions, it is possible that pDNA would be efficiently delivered to DC in vivo by polyplex formation and the efficiency of direct priming in the induction of immune responses might be improved. Our previous study also demonstrated prolonged retention of pDNA in the treated skins and enhanced accumulation of pDNA in the regional lymph nodes, which might be involved in increased direct interaction of pDNA with DC.

Another possible factor for improved antibody production may be induction of substance P in the treated skins. It is reported that cationic peptide/molecules stimulate sensory nerves in dermis, resulted in releasing substance P and stimulating mast cells [22–24]. Therefore, mBSA, cationic macromolecule used in this study, might have similar biological functions. Substance P can stimulate keratinocytes and activation of mast cells also may affect induction of immune responses. Even if this was the case, the level of Substance P or mast cell activation was not so high because we observed little edema or damage in the treated skins under the microscope.

The detailed mechanism for the accumulation of DC and LC induced by polyplex injection is unknown. KC participates in cutaneous immune responses by producing various cytokines. Topical exposure of mice to contact allergens and skin irritants is known to stimulate the upregulated expression of various epidermal cytokines, including IL-1β, IL-6, TNF-α, GM-CSF and macrophage inflammatory protein 2 (MIP-2). Among them, IL-1β, TNF-α and IL-6 are known to provide mandatory signals for the mobilization of DC and LC. In the epidermis, KC is the main source of TNF-α, although other cell types may also produce a small amount of this cytokine. Immature DC express CC chemokine receptor 6 (CCR6). The ligands for CCR6, MIP-3α and defensins-β, are expressed in KC and migration of DC occurs depending on the ligand-receptor interaction. It has been reported that the expression of MIP-3α and defensins-β are enhanced by TNF-α from KC [25,26]. TNF-α also stimulates vascular endothelial cells in inflammatory sites and increases the expression of vascular cell adhesion molecule-1 (VCAM-1), which can facilitate DC accumulation in local tissue from the blood circulation. These processes would be involved in the DC accumulation observed in the present study.

A number of mechanisms of TNF-α production from KC have been reported [27–29]. KC constitutively express various members of the toll-like receptor (TLR) family, such as TLR1, TLR2, TLR3, TLR5 and TLR9 but not TLR4, TLR6, TLR7, TLR8 or TLR10. It is well known that the so-called CpG motifs in bacterial DNA, such as pDNA, are recognized by TLR9 and trigger signaling pathways that activate various transcription factors, including NF-κB and activator protein-1. These results suggest that the production of TNF-α might be due to CpG motif recognition by TLR9 expressed by KC. Polyplex formation would enhance cellular uptake of pDNA and its stability compared with naked pDNA. This effect would not be specific to mBSA, the cationic carrier used in this study, because the production of TNF-α from

KC was also detected when we use other cationic macromolecules, such as poly L-lysine (data not shown), to prepare the polyplex in our preliminary study.

Endogenous and exogenous antigens in DC followed by processing to antigen peptide are present on MHC class I and II molecule, respectively. The presentation of antigen peptide on MHC class II leads to antibody production following proliferation of $CD4^+$ helper T cells. We believe that enhanced antibody production by polyplex-based DNA vaccination might be due, at least in part, to increased direct delivery of pDNA to DC in the treated skin. After endogenous antigen is expressed and secreted from DC, the DC itself or surrounding DC would be taken up by the antigen in the injection site and presented to MHC class II. It is also known that the endogenous antigen is also directly delivered via the MHC class II-restricted pathway in the cells [30–35].

It has been reported that the routes and methods of pDNA delivery affect the immunological consequences following DNA vaccination [36–38]. For example, intradermal administration has been shown to be more efficient than intramuscular administration as far as the induction of humoral immune response is concerned. pDNA delivered to the skin by intradermal injection or gene gun appears to activate the Th2 polarized response, whereas intramuscular injection of pDNA predominantly induces the Th1 response. The selection of pDNA formulations is also one of the most important factors for the determination of immune responses. It has been reported that adjuvants and delivery systems, such as cationic macroparticles [39,40], chitosan (in a case of mucosal vaccination) [41,42] and lipid vesicles [43,44], can be used not only to increase the strength of the immune response, but also to influence the types of induced cellular and antibody responses. Manipulation of DC migration using various chemokines, such as MIP-1α, regulated on activation normal T cell expressed and secreted (RANTES) is also a promising approach [45,46]. The present study has demonstrated that polyplex-based DNA vaccination is another option for manipulating antigen-specific immune responses.

In conclusion, we have demonstrated that the immune responses can be biased towards the antibody production by polyplex-based DNA vaccination through manipulation of not only pDNA disposition and expression but also dendritic cell migration. We also considered that the inducibility for Th-2 type response is the advantage of polyplex-based DNA vaccination.

Acknowledgements

This work was supported in part by a Grant-in-Aid for Scientific Research from the Ministry of Education, Culture, Sports, Science and Technology of Japan, by Uehara Memorial Foundation and 21st Century COE Program "Knowledge Information Infrastructure for Genome Science".

References

[1] Tang DC, DeVit M, Johnston SA. Genetic immunization is a simple method for eliciting an immune response. Nature 1992;356(6365):152–4.
[2] Ulmer JB, Donnelly JJ, Parker SE, Rhodes GH, Felgner PL, Dwarki VJ, et al. Heterologous protection against influenza by injection of DNA encoding a viral protein. Science 1993;259(5102):1745–9.
[3] Porgador A, Irvine KR, Iwasaki A, Barber BH, Restifo NP, Germain RN. Predominant role for directly transfected dendritic cells in antigen presentation to CD8+ T cells after gene gun immunization. J Exp Med 1998;188(6):1075–82.
[4] Shedlock DJ, Weiner DB. DNA vaccination: antigen presentation and the induction of immunity. J Leukoc Biol 2000;68(6):793–806.
[5] Maecker HT, Umetsu DT, DeKruyff RH, Levy S. DNA vaccination with cytokine fusion constructs biases the immune response to ovalbumin. Vaccine 1997;15(15):1687–96.
[6] Gilkeson GS, Pippen AM, Pisetsky DS. Induction of cross-reactive anti-dsDNA antibodies in preautoimmune NZB/NZW mice by immunization with bacterial DNA. J Clin Invest 1995;95(3):1398–402.
[7] Gilkeson GS, Ruiz P, Pippen AM, Alexander AL, Lefkowith JB, Pisetsky DS. Modulation of renal disease in autoimmune NZB/NZW mice by immunization with bacterial DNA. J Exp Med 1996;183(4):1389–97.
[8] Uchi H, Terao H, Koga T, Furue M. Cytokines and chemokines in the epidermis. J Dermatol Sci 2000;24(Suppl. 1):S29–38.
[9] Wang B, Amerio P, Sauder DN. Role of cytokines in epidermal Langerhans cell migration. J Leukoc Biol 1999;66(1):33–9.
[10] Cumberbatch M, Dearman RJ, Kimber I. Langerhans cells require signals from both tumour necrosis factor-alpha and interleukin-1 beta for migration. Immunology 1997;92(3):388–95.
[11] Cotten M, Baker A, Saltik M, Wagner E, Buschle M. Lipopolysaccharide is a frequent contaminant of plasmid DNA preparations and can be toxic to primary human cells in the presence of adenovirus. Gene Ther 1994;1(4):239–46.
[12] Hartmann G, Krieg AM. CpG DNA and LPS induce distinct patterns of activation in human monocytes. Gene Ther 1999;6(5):893–903.
[13] Mandell JD, Hershey AD. A fractionating column for analysis of nucleic acids. Anal Biochem 1960;1:66–77.
[14] Chonn A, Semple SC, Cullis PR. Association of blood proteins with large unilamellar liposomes in vivo. Relation to circulation lifetimes. J Biol Chem 1992;267(26):18759–65.
[15] Ito D, Ogasawara K, Iwabuchi K, Inuyama Y, Onoe K. Induction of CTL responses by simultaneous administration of liposomal peptide vaccine with anti-CD40 and anti-CTLA-4 mAb. J Immunol 2000;164(3):1230–5.
[16] McNeela EA, Mills KH. Manipulating the immune system: humoral versus cell-mediated immunity. Adv Drug Deliv Rev 2001; 51(1–3):43–54.
[17] Donnelly JJ, Ulmer JB, Shiver JW, Liu MA. DNA vaccines. Annu Rev Immunol 1997;15:617–48.
[18] Howard KA, Alpar HO. The development of polyplex-based DNA vaccines. J Drug Target 2002;10(2):143–51.
[19] Howard KA, Li XW, Somavarapu S, Singh J, Green N, Atuah KN, et al. Formulation of a microparticle carrier for oral polyplex-based DNA vaccines. Biochim Biophys Acta 2004;1674(2):149–57.
[20] Schlecht G, Leclerc C, Dadaglio G. Induction of CTL and nonpolarized Th cell responses by CD8alpha(+) and CD8alpha(−) dendritic cells. J Immunol 2001;167(8):4215–21, 15.
[21] Kawase A, Kobayashi N, Isaji K, Nishikawa M, Takakura Y. Manipulation of local disposition and gene expression characteristics of plasmid DNA following intramuscular administration by complexation with cationic macromolecule. Int J Pharm 2005;293(1–2):291–301, 11.
[22] Coyle AJ, Perretti F, Manzini S, Irvin CG. Cationic protein-induced sensory nerve activation: role of substance P in airway

hyperresponsiveness and plasma protein extravasation. J Clin Invest 1994;94(6):2301–6.
[23] Okayama Y, el-Lati SG, Leiferman KM, Church MK. Eosinophil granule proteins inhibit substance P-induced histamine release from human skin mast cells. J Allergy Clin Immunol 1994;93(5):900–9.
[24] Manske JM, Hanson SE. Substance-P-mediated immunomodulation of tumor growth in a murine model. Neuroimmunomodulation 2005;12(4):201–10.
[25] Tohyama M, Shirakara Y, Yamasaki K, Sayama K, Hashimoto K. Differentiated keratinocytes are responsible for TNF-alpha regulated production of macrophage inflammatory protein 3alpha/CCL20, a potent chemokine for Langerhans cells. J Dermatol Sci 2001;27(2):130–9.
[26] Dieu-Nosjean MC, Massacrier C, Homey B, Vanbervliet B, Pin JJ, Vicari A, et al. Macrophage inflammatory protein 3alpha is expressed at inflamed epithelial surfaces and is the most potent chemokine known in attracting Langerhans cell precursors. J Exp Med 2000;192(5):705–18.
[27] Mempel M, Voelcker V, Kollisch G, Plank C, Rad R, Gerhard M, et al. Toll-like receptor expression in human keratinocytes: nuclear factor kappaB controlled gene activation by Staphylococcus aureus is toll-like receptor 2 but not toll-like receptor 4 or platelet activating factor receptor dependent. J Invest Dermatol 2003;121(6):1389–96.
[28] Krieg AM. CpG motifs in bacterial DNA and their immune effects. Annu Rev Immunol 2002;20:709–60.
[29] Zhao Q, Temsamani J, Zhou RZ, Agrawal S. Pattern and kinetics of cytokine production following administration of phosphorothioate oligonucleotides in mice. Antisense Nucleic Acid Drug Dev 1997;7(5):495–502.
[30] Nuchtern JG, Biddison WE, Klausner RD. Class II MHC molecules can use the endogenous pathway of antigen presentation. Nature 1990;343(6253):74–6.
[31] Sant AJ. Endogenous antigen presentation by MHC class II molecules. Immunol Res 1994;13(4):253–67.
[32] Oxenius AM, Bachmann F, Ashton-Rickardt PG, Tonegawa S, Zinkernagel RM, Hengartner H. Presentation of endogenous viral proteins in association with major histocompatibility complex class II: on the role of intracellular compartmentalization, invariant chain and the TAP transporter system. Eur J Immunol 1995;25(12):3402–11.
[33] Lechler R, Aichinger G, Lightstone L. The endogenous pathway of MHC class II antigen presentation. Immunol Rev 1996;151:51–79.
[34] Koch N, van Driel IR, Gleeson PA. Hijacking a chaperone: manipulation of the MHC class II presentation pathway. Immunol Today 2000;21(11):546–50.
[35] Qi L, Ostrand-Rosenberg S. MHC class II presentation of endogenous tumor antigen by cellular vaccines depends on the endocytic pathway but not H2-M. Traffic 2000;1(2):152–60.
[36] Pertmer TM, Roberts TR, Haynes JR. Influenza virus nucleoprotein-specific immunoglobulin G subclass and cytokine responses elicited by DNA vaccination are dependent on the route of vector DNA delivery. J Virol 1996;70(9):6119–25.
[37] Feltquate DM, Heaney S, Webster RG, Robinson HL. Different T helper cell types and antibody isotypes generated by saline and gene gun DNA immunization. J Immunol 1997;158(5):2278–84.
[38] Yoshida A, Nagata T, Uchijima M, Higashi T, Koide Y. Advantage of gene gun-mediated over intramuscular inoculation of plasmid DNA vaccine in reproducible induction of specific immune responses. Vaccine 2000;18(17):1725–9.
[39] Singh M, Briones M, Ott G, O'Hagan D. Cationic microparticles: A potent delivery system for DNA vaccines. Proc Natl Acad Sci USA 2000;97(2):811–6.
[40] Denis-Mize KS, Dupuis M, MacKichan ML, Singh M, Doe B, O'Hagan D, et al. Plasmid DNA adsorbed onto cationic microparticles mediates target gene expression and antigen presentation by dendritic cells. Gene Ther 2000;7(24):2105–12.
[41] McNeela EA, O'Connor D, Jabbal-Gill I, Illum L, Davis SS, Pizza M, et al. A mucosal vaccine against diphtheria: formulation of cross reacting material (CRM(197)) of diphtheria toxin with chitosan enhances local and systemic antibody and Th2 responses following nasal delivery. Vaccine 2000;19(9–10):1188–98.
[42] Jabbal-Gill I, Fisher AN, Rappuoli R, Davis SS, Illum L. Stimulation of mucosal and systemic antibody responses against Bordetella pertussis filamentous haemagglutinin and recombinant pertussis toxin after nasal administration with chitosan in mice. Vaccine 1998;16(20):2039–46.
[43] Bramwell VW, Eyles JE, Somavarapu S, Alpar HO. Liposome/DNA complexes coated with biodegradable PLA improve immune responses to plasmid encoding hepatitis B surface antigen. Immunology 2002;106(3):412–8.
[44] Klavinskis LS, Gao L, Barnfield C, Lehner T, Parker S. Mucosal immunization with DNA-liposome complexes. Vaccine 1997;15(8):818–20.
[45] Yamazaki S, Yokozeki H, Satoh T, Katayama I, Nishioka K. TNF-alpha, RANTES, and MCP-1 are major chemoattractants of murine Langerhans cells to the regional lymph nodes. Exp Dermatol 1998;7(1):35–41.
[46] Sozzani S, Sallusto F, Luini W, Zhou D, Piemonti L, Allavena P, et al. Migration of dendritic cells in response to formyl peptides, C5a, and a distinct set of chemokines. J Immunol 1995;155(7):3292–5.

Gene Therapy (2005) 12, 607–616

www.nature.com/gt

RESEARCH ARTICLE

Hepatocyte-targeted gene transfer by combination of vascularly delivered plasmid DNA and in vivo electroporation

M Sakai[1], M Nishikawa[2], O Thanaketpaisarn[1], F Yamashita[1] and M Hashida[1]

[1]Department of Drug Delivery Research, Graduate School of Pharmaceutical Sciences, Kyoto University, Sakyo-ku, Kyoto, Japan; and [2]Department of Biopharmaceutics and Drug Metabolism, Graduate School of Pharmaceutical Sciences, Kyoto University, Sakyo-ku, Kyoto, Japan

To increase transgene expression in the liver, electric pulses were applied to the left lateral lobe after intravenous injection of naked plasmid DNA (pDNA) or pDNA/liver targeting vector complex prepared with galactosylated poly(L-lysine) or galactosylated polyethyleneimine. Electroporation (250 V/cm, 5 ms/pulse, 12 pulses, 4 Hz) after naked pDNA injection dramatically increased the expression up to 200 000-fold; the expression level obtained was significantly greater than that achieved by the combination of pDNA/vector complex and electroporation. We clearly demonstrated that the expression was dependent on the plasma concentration of pDNA at the time when the electric pulses were applied. Separation of liver cells revealed that the distribution of naked pDNA as well as transgene expression was largely selective to hepatocytes in the electroporated lobe. The number of cells expressing transgene product using vascularly administered naked pDNA followed by electroporation was significantly ($P<0.01$) greater and more widespread than that obtained by local injection of naked pDNA. These results indicate that the application of in vivo electroporation to vascularly administered naked pDNA is a useful gene transfer approach to a large number of hepatocytes.

Gene Therapy (2005) **12**, 607–616. doi:10.1038/sj.gt.3302435
Published online 23 December 2004

Keywords: *electroporation; tissue distribution; liver; hepatocytes; asialoglycoprotein receptor*

Introduction

The success of *in vivo* gene therapy relies on the development of vectors that can selectively and effectively deliver a therapeutic gene to the target with minimal toxicity. Nonviral vectors such as naked plasmid DNA (pDNA) and its complex with a cationic vector, with or without a specific ligand, has advantages over viral vectors in terms of the simplicity of use, ease of large-scale production and lack of a specific immune response.[1] However, the low efficiency of transgene expression needs to be improved. We have developed various delivery systems for pDNA, incorporating galactose[2,3] or mannose[4] to achieve cell-specific targeting to hepatocytes or liver nonparenchymal cells (NPC), respectively. These vectors were highly effective in delivering pDNA to the cells, but the transfection efficiency still needs to be improved.

A major barrier for successful *in vivo* gene transfer is the poor membrane permeability of pDNA as well as its lysosomal degradation within cells after entrance via endocytosis. Recently, various physical approaches such as electroporation,[5] sonoporation,[6] and hydrodynamic or hydrostatic pressure by large-volume injection[7,8] have been developed for improving transgene expression by nonviral vectors. Among these approaches, *in vivo* electroporation, which is suggested to transiently create pores on cell membranes[9] and has been tested in clinical trials for cancer chemotherapy,[10,11] has been extensively studied as a method to increase transgene expression by naked pDNA after local injection into the interstitial spaces of tissues. *In vivo* electroporation has been applied to various tissues including skin,[5] liver,[12,13] melanoma,[14] and muscle.[15] Generally speaking, electroporation increases transgene expression up to 1000-fold compared with that obtained with simple naked pDNA injection. However, the application of *in vivo* electroporation has been limited to locally injected pDNA, where the distribution of transgene-expressing cells is limited to a narrow area around the injection site.[16] Although the application of electric pulses to locally injected pDNA can increase the area of those cells, the spread is still limited due to the huge size of pDNA.

Vascularly administered pDNA can be distributed to a greater number of cells than locally injected pDNA. Therefore, the application of electroporation to vascularly administered pDNA could achieve transgene expression in a large target cell population. Gene therapy for the deficiency of an intracellular enzyme or structural protein requires functional restoration at the cell level, so the number of cells producing the transgene would be a major factor determining the therapeutic efficacy of the gene transfer approach. Although the application of electroporation after systemic administration of pDNA

Correspondence: Dr M Nishikawa, Department of Biopharmaceutics and Drug Metabolism, Graduate School of Pharmaceutical Sciences, Kyoto University, Sakyo-ku, Kyoto 606-8501, Japan
Received 2 January 2004; accepted 4 October 2004; published online 23 December 2004

can be a promising technique to achieve this, it has received little attention so far. Recently, Liu and Huang[17] published a report on electroporation-mediated gene transfer to the liver after intravenous injection of naked pDNA. They found that electroporation combined with intravenous naked pDNA can be a good method of achieving gene transfer to a larger number of liver cells compared with locally injected pDNA. However, the characteristics of gene transfer and its underlying mechanism need to be investigated to optimize this technique, in which electroporation is applied to a tissue after vascularly administered pDNA. Due to its strong negative charge, naked pDNA is rapidly taken up by the liver NPC after intravenous injection,[18,19] which results in no significant transgene expression in the organ. This uptake rapidly reduces the concentration of pDNA within the circulation. Although the results obtained by Liu and Huang[17] suggest that the distribution of pDNA would be altered by electroporation, little is known about the tissue distribution of pDNA. Targeted delivery of pDNA to hepatocytes can be achieved by galactosylated vectors, but the combined use of targeted delivery of pDNA using vectors and electroporation has not been examined so far.

We hypothesized that the application of electric pulses alters the distribution of pDNA at the site of electroporation. The liver is composed of various types of cells including hepatocytes, sinusoidal endothelial cells and Kupffer cells, and, in many genetic deficiencies such as ornithine transcarbamylase deficiency, hepatocytes can be the target of gene transfer. Therefore, we tried to achieve efficient gene transfer to hepatocytes by applying electroporation to intravenously administered pDNA. We injected pDNA into the tail vein of mice in the free form (naked pDNA) or in the complex form with a hepatocyte-targeted vector: galactosylated poly(L-lysine) (Gal-PLL)[20] or galactosylated polyethyleneimine (Gal-PEI).[3] First, the effect of electroporation was examined on the whole-body distribution of naked pDNA and pDNA/Gal-PLL using ^{32}P-labeled pDNA. Then transgene expression in the liver was evaluated after administering intravenous pDNA or its complex followed by electroporation onto the liver. As naked pDNA showed the greatest transgene expression among the vectors examined, the characteristics of the expression by naked pDNA with electroporation were investigated in detail in terms of the distribution of pDNA and transfected cells within the electroporated lobe. We report here that intravenous naked pDNA injection followed by hepatic electroporation is a good way of achieving selective gene transfer to a number of hepatocytes with a higher transfection efficiency than that offered by vector-targeted gene transfer. Hepatocytes are found to be more susceptible to the effects of electroporation than other liver NPC, and the delivery of pDNA and transgene expression are selectively improved in hepatocytes by electroporation.

Results

Effect of electroporation on pharmacokinetics of pDNA and its complex

After intravenous injection, ^{32}P-pDNA is preferentially taken up by liver NPC,[18,19] whereas a large fraction of ^{32}P-pDNA/Gal-PLL is delivered to hepatocytes through asialoglycoprotein receptor-mediated endocytosis.[20] Without electroporation, both naked ^{32}P-pDNA and ^{32}P-pDNA/Gal-PLL showed similar pharmacokinetic profiles to those reported previously; ^{32}P-radioactivity quickly disappeared from the blood circulation and accumulated in the liver (Figures 1 and 2). When naked ^{32}P-pDNA was injected, the radioactivity in the liver quickly decreased with time (Figure 1), reflecting its degradation by the organ. A set of electric pulses (250 V/cm, 5 ms/pulse, 12 pulses, 4 Hz) was applied to the left lateral lobe of the liver at 30 s after intravenous injection of either naked ^{32}P-pDNA (Figure 1) or ^{32}P-pDNA/Gal-PLL (Figure 2). No significant changes in the plasma concentration and liver accumulation of ^{32}P-radioactivity were detected in either case.

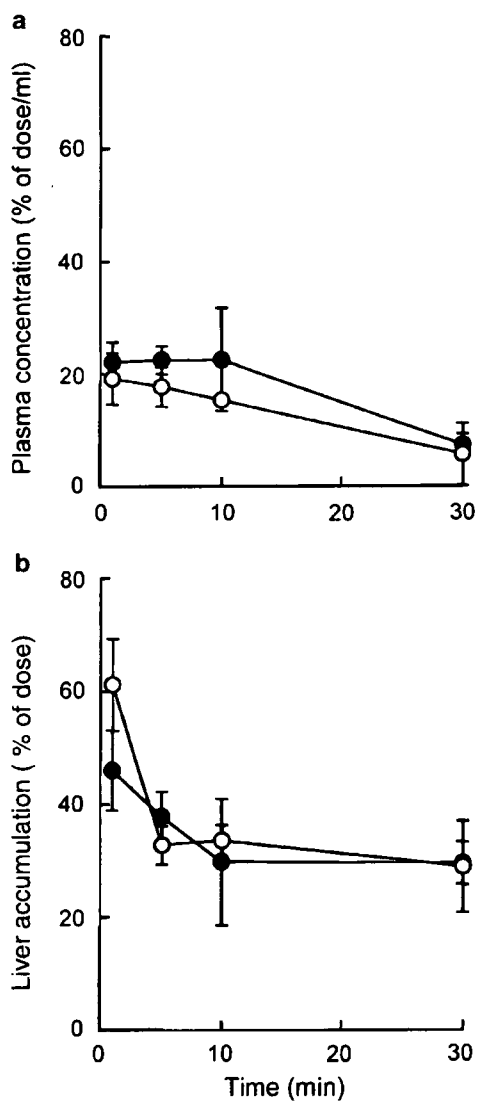

Figure 1 Plasma concentration (a) and liver accumulation (b) of ^{32}P-radioactivity after injection of naked ^{32}P-pDNA with or without electroporation. Naked ^{32}P-pDNA was injected into the tail vein at a dose of 25 μg/mouse, and electric pulses (250 V/cm, 5 ms/pulse, 12 pulses, 4 Hz) were applied to the left lateral lobe of the liver at 30 s after injection. Results are expressed as the mean ± s.d. of three mice. (○) injection only; (●) electroporated.

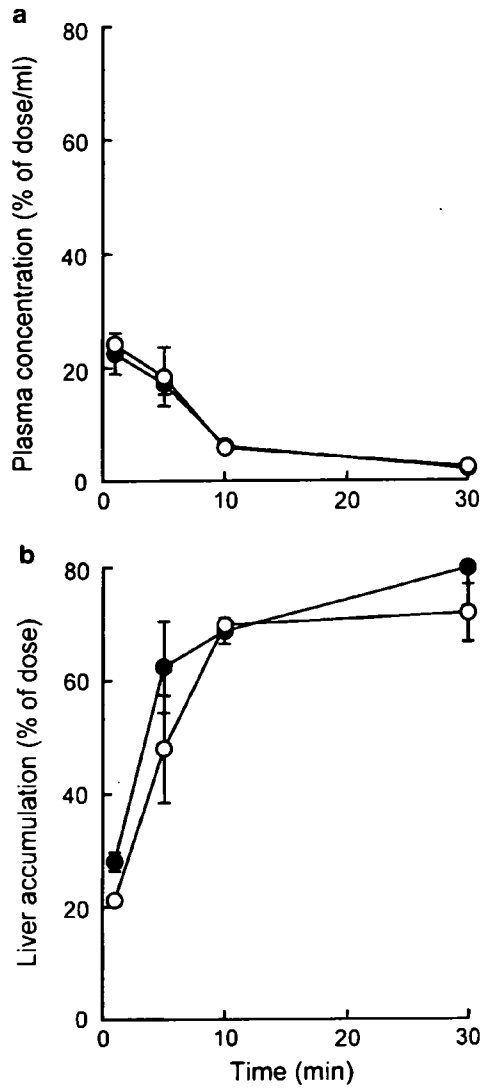

Figure 2 Plasma concentration (a) and liver accumulation (b) of ^{32}P-radioactivity after injection of ^{32}P-pDNA/Gal-PLL complex with or without electroporation. ^{32}P-pDNA/Gal-PLL complex (N/P ratio of 2.4) was injected into the tail vein at a dose of 25 μg/mouse, and electric pulses (250 V/cm, 5 ms/pulse, 12 pulses, 4 Hz) were applied to the left lateral lobe of the liver at 30 s after injection. Results are expressed as the mean ± s.d. of three mice. (○) Injection only; (●) electroporated.

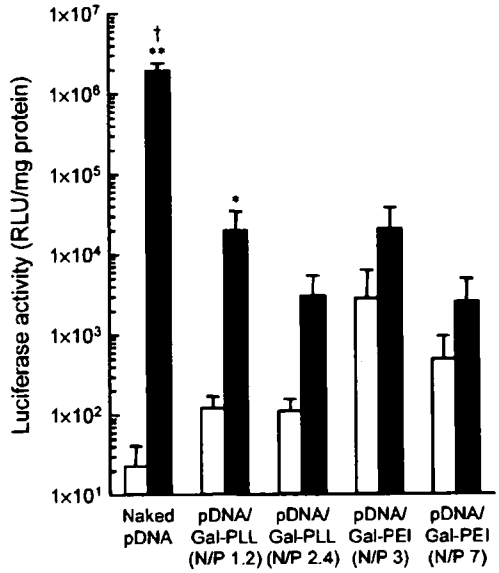

*Figure 3 Transgene expression after injection of naked pDNA, pDNA/Gal-PLL or pDNA/Gal-PEI complex with or without electroporation. pDNA complex was injected into the tail vein at a dose of 25 μg/mouse, and electric pulses (250 V/cm, 5 ms/pulse, 12 pulses, 4 Hz) were applied to the left lateral lobe of the liver at 30 s after injection. Results are expressed as the mean ± s.d. of at least three mice. (open bar) injection only; (closed bar) electroporated. *,**Statistically significant difference compared to the expression without electroporation (*$P<0.01$, **$P<0.001$). †Statistically significant difference between naked pDNA and all other groups ($P<0.001$).*

Effect of electroporation on transgene expression by vascular pDNA and its complex

Transgene expression was detected at 6 h after injection of 25 μg pDNA or its complex in the following experiments. The electroporation parameters were fixed as follows unless otherwise indicated: electric field, 250 V/cm; duration of each pulse, 5 ms; number of pulses, 12; frequency of pulses, 4 Hz; timing of pulses, 30 s after injection; site of electroporation, the left lateral lobe.

No significant transgene expression was detected in the liver after intravenous injection of naked pDNA (Figure 3). pDNA/Gal-PLL or pDNA/Gal-PEI complex showed detectable transgene expression in the liver. However, the expression level obtained was not very high, probably due to the small dose of pDNA injected. The application of electric pulses increased the expression in the electroporated lobe of the liver against any vector used (Figure 3). However, the enhancement ratio and the final level of transgene expression varied among the vectors. Naked pDNA showed the greatest enhancement ratio in transgene expression and the greatest expression level. The expression in the electroporated lobe increased up to 200 000-fold. The level of expression (about 2×10^6 RLU/mg protein) was about 100-fold greater than that obtained after the injection of pDNA complex followed by electroporation.

To confirm the effect of electroporation on the receptor-mediated gene transfer, transgene expression by naked pDNA or pDNA/Gal-PLL was examined in HepG2 cells, a human hepatoma cell line expressing asialoglycoprotein receptors. Again, electroporation increased the expression to 4500-fold for naked pDNA and nine-fold for pDNA/Gal-PLL (data not shown), suggesting that the free form of pDNA is more effective than its complexed form for transgene expression once it enters into the cytoplasm of cells.

Effect of strength of electric field on transgene expression by vascular naked pDNA

Figure 4 shows the transgene expression in the electroporated lobe and other lobes after intravenous injection of naked pDNA followed by electroporation with various electric fields from 50 to 500 V/cm. At any

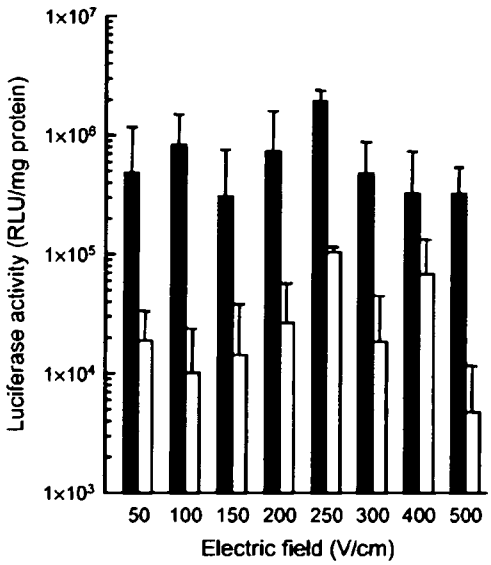

Figure 4 Effect of the strength of electric field on transgene expression after injection of naked pDNA followed by electroporation. Naked pDNA was injected into the tail vein at a dose of 25 μg/mouse, and electric pulses (50–500 V/cm, 5 ms/pulse, 12 pulses, 4 Hz) were applied to the left lateral lobe of the liver at 30 s after injection. Results are expressed as the mean ± s.d. of at least three mice. (closed bar) electroporated lobe; (open bar) nonelectroporated lobes.

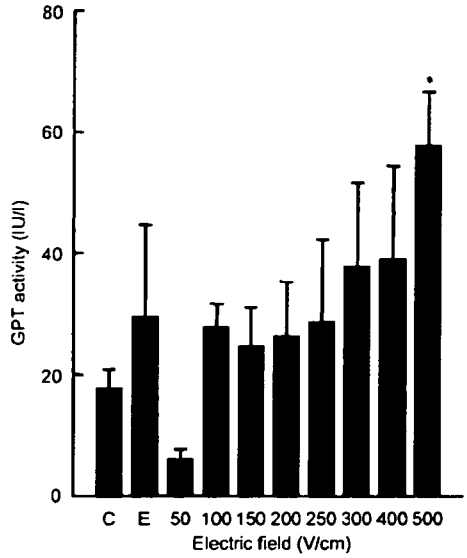

*Figure 5 GPT activity in mouse plasma after injection of naked pDNA followed by electroporation. Naked pDNA was injected into the tail vein at a dose of 25 μg/mouse, and electric pulses (50–500 V/cm, 5 ms/pulse, 12 pulses, 4 Hz) were applied to the left lateral lobe of the liver at 30 s after injection. Results are expressed as the mean ± s.d. of at least three mice. *Statistically significant difference compared to the injection only group ($P < 0.01$). C, control, electrodes were not applied to the liver; E, electrodes were applied, but pulses were not delivered.*

electric field examined, high transgene expression was obtained in the electroporated lobe, with a peak value at 250 V/cm. The expression in the nonelectroporated lobes was greater than that in the mouse liver receiving no electroporation shown in Figure 3. These results suggest that the electric pulses applied to the left lateral lobe of the liver have some influence on transgene expression in other lobes. However, there was no significant transgene expression in other organs such as the kidney, spleen, lung and heart (< 100 RLU/mg protein; data not shown).

Glutamic pyruvic transferase (GPT) activity in plasma rose slightly as the electric field of the pulses increased (Figure 5). However, the activity was still low even at the highest electric field of 500 V/cm. The liver surface receiving the pulses did not show any significant changes following electroporation (data not shown).

Correlation between transgene expression and plasma concentration of pDNA

Figure 6 shows the effect of the time interval between the intravenous injection of naked pDNA and electroporation on transgene expression in the electroporated lobe. Transgene expression decreased with the interval, and became undetectable when electric pulses were applied with an interval of 20 min or longer.

Figure 7a shows the agarose gel electrophoresis of pDNA recovered from mouse plasma after intravenous injection of naked pDNA. The amounts of pDNA in supercoiled (SC), open circular (OC) and linear (L) forms were measured by densitometric analysis, and the results are summarized in Figure 7b. pDNA within the blood circulation rapidly changed its structure and decreased with time. No intact pDNA could be detected in plasma

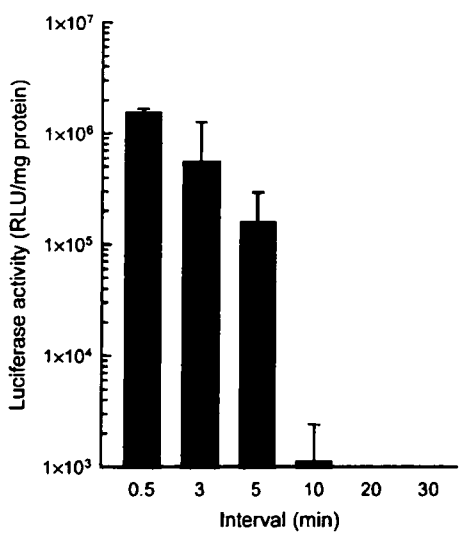

Figure 6 Effect of time interval between naked pDNA injection and electroporation on transgene expression. Naked pDNA was injected into the tail vein at a dose of 25 μg/mouse, and electric pulses (50–500 V/cm, 5 ms/pulse, 12 pulses, 4 Hz) were applied to the left lateral lobe of the liver at different intervals. Results are expressed as the mean ± s.d. of at least three mice.

at 5 min and beyond. The concentration of pDNA in plasma at electroporation correlated well with the final expression in the liver (Figure 8), suggesting that pDNA in the circulation, not captured by liver cells, is responsible for transgene expression.

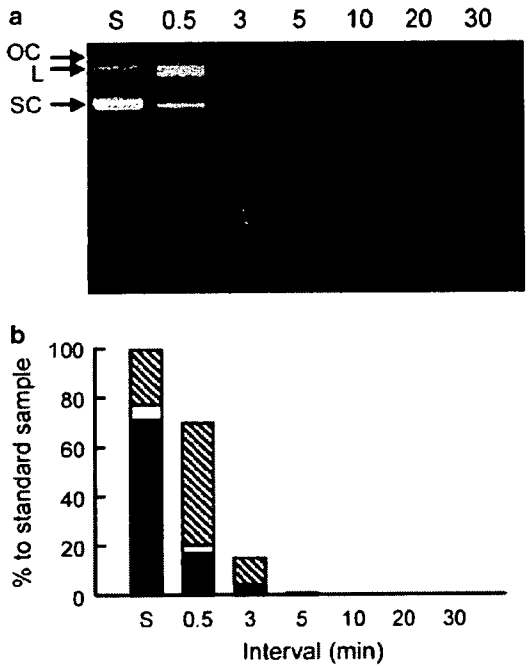

Figure 7 Stability of naked pDNA after injection into mice. (a) Naked pDNA was injected into the tail vein at a dose of 25 μg/mouse, and pDNA was recovered from mouse blood at indicated time points after injection, electrophoresed on agarose gel and visualized with ethidium bromide. (b) The amounts of pDNA in supercoiled, open circular and linear forms were measured by densitometric analysis. SC (closed bar), supercoiled; OC (open bar), open circular; L (striped bar), linear; S, standard pDNA (0.5 μg pDNA).

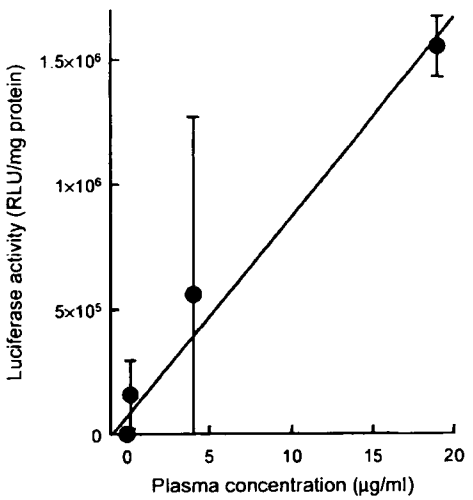

Figure 8 Relation between transgene expression and the plasma concentration of pDNA at electroporation. Transgene expression in the electroporated lobe of the liver (Figure 6) was plotted against the total concentration of pDNA (Figure 7b). Experimental details are described in the legends of Figures 6 and 7.

Cellular distribution of radioactivity and transgene expression in mouse liver after injection of naked pDNA followed by electroporation

Naked pDNA is extensively taken up by liver NPC via mechanism(s) like scavenger receptors.[18,21] In the nonelectroporated lobes of the liver, ^{32}P-radioactivity preferentially distributed to NPC rather than hepatocytes (parenchymal cells, PC) (Figure 9a). NPC uptake was about three-fold greater than PC uptake on a cell number basis, with a PC/NPC ratio of 0.35. The PC/NPC ratio increased in the electroporated lobe to 0.78, indicating that the distribution of pDNA shifted from NPC to PC by electroporation.

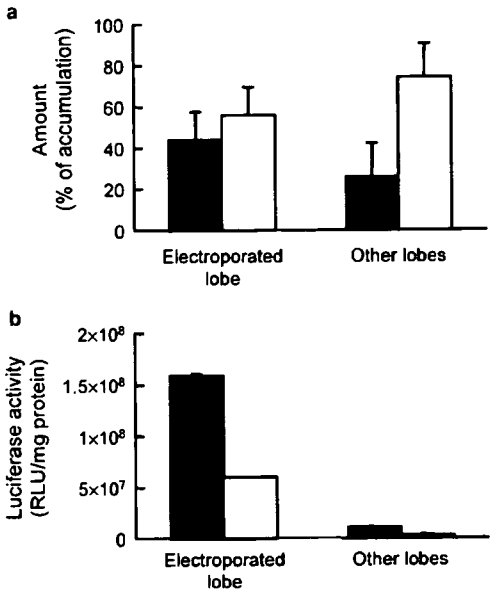

Figure 9 Distribution of ^{32}P-radioactivity (a) and luciferase activity (b) in the electroporated and nonelectroporated lobes after injection of naked pDNA followed by electroporation. Naked ^{32}P-pDNA or pDNA was injected into the tail vein at a dose of 25 μg/mouse, and electric pulses (250 V/cm, 5 ms/pulse, 12 pulses, 4 Hz) were applied to the left lateral lobe of the liver at 30 s after injection. PC (closed bar) and NPC (open bar) were separated and ^{32}P-radioactivity (a) or luciferase activity (b) in these cell fractions was assayed. Results are expressed as the mean ± s.d. of at least three mice.

As shown in Figure 4, transgene expression was very high in the electroporated lobe. Separation of the cells in the lobe clearly demonstrated that the expression in PC was significantly ($P<0.01$) greater than that in NPC (Figure 9b).

Analysis of the number of cells expressing transgene product

Figure 10b and c shows typical liver tissues receiving an intravenous injection of naked β-galactosidase-expressing pDNA followed by electroporation. For comparison, naked pDNA was directly injected into the left lateral lobe of the liver (Figure 10a), which resulted in a very localized distribution of β-galactosidase-positive cells near the injection site (arrow). Greater numbers of hepatocytes in a large area around the site of electroporation were transfected by intravenous naked pDNA followed by electroporation (Figure 10b and c).

To quantitatively evaluate the number of β-galactosidase-positive cells, we isolated hepatocytes from the left lateral lobe of the liver after administration of β-galactosidase-expressing pDNA to mice (Figure 10d).